Nonlinear Geometric Optics method based multi-scale numerical schemes for highly-oscillatory transport equations

Nicolas Crouseilles[*]   Shi Jin [†]   Mohammed Lemou[‡]

Contents

[*]Inria, IRMAR, University of Rennes 1, Rennes, France

[†]Department of Mathematics, University of Wisconsin-Madison, USA; Department of Mathematics, Institute of Natural Sciences, MOE-LSEC and SHL-MAC, Shanghai Jiao Tong University, Shanghai 200240, China (sjin@wisc.edu). This author's research was also supported by NSF grants 1522184, 1107291 (KI-Net) and NSFC grant 91330203.

[‡]CNRS, IRMAR, University of Rennes 1, Rennes, France

Abstract

We introduce a new numerical strategy to solve a class of oscillatory transport PDE models which is able to capture accurately the solutions without numerically resolving the high frequency oscillations *in both space and time*. Such PDE models arise in semiclassical modeling of quantum dynamics with band-crossings, and other highly oscillatory waves. Our first main idea is to use the nonlinear geometric optics ansatz, which builds the oscillatory phase into an independent variable. We then choose suitable initial data, based on the Chapman-Enskog expansion, for the new model. For a scalar model, we prove that so constructed model will have certain smoothness, and consequently, for a first order approximation scheme we prove uniform error estimates independent of the (possibly small) wave length. The method is extended to systems arising from a semiclassical model for surface hopping, a non-adiabatic quantum dynamic phenomenon. Numerous numerical examples demonstrate that the method has the desired properties.

1   Introduction

Many partial differential equations for high frequency waves, in particular, semiclassical models in quantum dynamics, take the form of systems of transport or Liouville equations with oscillatory source terms describing interband quantum transitions that are associated with chemical reactions, quantum tunnelling, Dirac points in graphene, etc. [33, 34, 6]. These terms contain important quantum information, such as Berry connection and Berry phase, which are associated with quantum Hall effects [39]. Solving such systems are computationally daunting since one needs to numerically resolve the small wave length (denoted by a small parameter ε in this paper), which can be prohibitively expansive.

To efficiently solve a quantum system, or more generally high frequency waves, a classical method is the geometric optics (GO) or WKB method, which approximates the amplitude by a transport equation and phase by (nonlinear) eiconal equation [32]. This method allows the computational mesh (Δx) and time step (Δt) independent of ε [15]. However the approximation is not valid beyond caustics, since the physically relevant solutions are multi-valued, rather than the viscosity, solutions to the eiconal equation [38, 22, 12, 24]. Even the multi-valued solutions do not describe accurately caustics, quantum tunnelling and other important non-adiabatic quantum phenomena. A more accurate method, called the Gaussian beam or Gaussian wave packet methods, originated independently in seismology [18, 35] and chemistry [17] communities (see also recent developments in the math community [36, 16, 29, 27, 30, 14]), are more accurate near caustics but need to use $\Delta x, \Delta t = O(\sqrt{\varepsilon})$, and have difficulties to handle singular potentials [26] and non-adiabatic band-crossing phenomena [25]. For recent overviews of computational high frequency waves and semiclassical methods for quantum dynamics, see [13, 23].

For problems that contain small or multiple time and space scales, another framework that has found many success in kinetic and hyperbolic problems is the

asymptotic-preserving (AP) *schemes* [20]. An AP scheme mimics the transition from a microscopic model to the macroscopic one in the discrete setting, and as a result the scheme can capture the macroscopic behavior correctly *without* resolving numerically the small, microscopic behavior, thus can be used for all range of ε with fixed Δx and Δt. Based on solving one model–the microscopic one, an AP scheme undergoes the numerical transition from the microscopic to the macroscopic scales *automatically* without the need to couple two different models at different scales, which is the bottleneck of most multiscale or multi-physical methods [11]. See recent reviews of AP methods in [21, 9]. For high frequency wave problems, the AP framework has found successes only in dealing with time oscillations, allowing $\Delta t \gg O(\varepsilon)$ [4, 19, 2, 3, 8, 7] for a number of physical problems. Nevertheless, for high frequency waves, the most difficult challenge is the spatial oscillations which unfortunately demands $\Delta x = O(\varepsilon)$, an impossible task in high space dimensions. One earlier work in this direction was in [1], by using the WKB-basis functions the method allows $\Delta x = O(1)$, but so far this approach has only been developed for one-dimensional stationary Schrödinger equation (without time oscillations).

In this paper we introduce a general AP approach to efficiently solve a family of oscillatory waves in which the phase oscillations depend *on both time and space*. The problem under study takes the following form

$$
\partial_t u + \sum_{k=1}^{d} A_k(x)\partial_{x_k} u + R(u) = \frac{i}{\varepsilon}E(t,x)Du + Cu, \qquad t \geq 0; \;\; x \in \Omega \subset \mathbb{R}^d,
$$
$$
u(0,x) = f_{in}(x, \beta(x)/\varepsilon), \quad x \in \Omega \subset \mathbb{R}^d,
$$
(1.1)

where $u = u(t,x) \in \mathbb{C}^n$, and A_k, D and C are given $n \times n$ real matrices. $R(u) : \mathbb{C}^n \mapsto \mathbb{C}^n$, is the source term independent of ε, the small dimensionless wave length. The quantity E is a real valued scalar function. The initial data f_{in} may have an oscillatory dependence with an initial phase $\beta(x)/\varepsilon$, and in this case we will assume that the dependence of f_{in} on this phase is periodic. Many semiclassal models for quantum dynamics may be written in this general form (see an example surface hopping [6], graphene [34], and quantum dynamics in periodic lattice [33]), in which $E \geq 0$ is the gap between different energy bands. Some high frequency wave equations also have the form of (1.1) [13]. In this paper, we assume periodic boundary condition in space such that $\Omega = [0,1]^d$, although the method can be extended to more general boundary conditions.

Our main idea is to use the *nonlinear geometric optics* (NGO), which has been widely studied at the theoretical level in the mathematical community last century for nonlinear hyperbolic conservation laws [10, 28, 31, 37]. The NGO approach builds the oscillatory phase as an independent variable. Specifically, one introduces a function $U : (t,x,\tau) \in (0,T) \times \mathbb{R}^d \times (0,2\pi) \to U(t,x,\tau) \in \mathbb{C}^n$, which is 2π-periodic with respect to the last variable $\tau \in (0,2\pi)$, and coincides with the solution u of (1.1) in the sense

$$
U(t,x,S(t,x)/\varepsilon) = u(t,x). \tag{1.2}
$$

We then transfer the original equation into a *linear* equation for the phase

3

$S(t, x)$–unlike in GO where the phase equation is the nonlinear eikonal equation which triggers caustics–coupled with an equation on the profile U. The main interest of our reformulation is twofold. First the equation for S is linear and does not depend on ε, which makes its numerical approximation simple, accurate and inexpensive. Second, thanks to the additional degree of freedom in U, one can, and *needs to*, choose suitable initial data such that $U(t, x, \tau)$ is uniformly bounded in ε up to certain order of derivatives in time and space, which can then be solved numerically efficiently: such initial data can be generated by utilizing the classical Chapman-Enskog expansion [5] as was done in [7, 8] to efficiently compute the time oscillations. As a result, our method is AP, *in both space and time*, which allows correct solutions even when $\Delta x, \Delta t \gg O(\varepsilon)$.

The paper is organized as follows. In section 2, we present in details the strategy for highly oscillatory scalar equations in one dimension. In particular we reformulate the problem into a new one with an additional dependence on a well-chosen oscillation phase. We prove that this augmented problem is smooth enough in both space and time with respect to the oscillation parameter. Based on this reformulation, we construct a numerical scheme for which we prove that the order of accuracy is also uniform in ε. Numerical results are performed to assert the efficiency of our method. Then, in section 3, we extend the strategy to a class of oscillatory hyperbolic systems with an application to a semiclassical surface hopping model. A conclusion is finally given in section 4.

We remark that our approach, although presented here only in one space dimension, can be generalized to higher space dimension straightforwardly. This will be the subject of a future work.

2   One dimensional scalar equations

As an illustrative example, we first consider the following model satisfied by $u(t, x) \in \mathbb{C}$, $x \in [0, 1]$, $t \geq 0$,

$$\partial_t u + c(x)\partial_x u + r(u) = \frac{ia(x)}{\varepsilon}u, \qquad u(0, x) = u_0(x), \tag{2.1}$$

where the functions u_0, a, c and r are given. Periodic boundary conditions are also considered in space. In some cases, we will allow the initial data to be oscillatory

$$u_0(x) = f_{in}(x, \beta(x)/\varepsilon) \equiv f_{in}(x, \tau) \qquad \text{with} \quad \tau = \frac{\beta(x)}{\varepsilon},$$

where β is a given function and f_{in} is supposed to be periodic with respect to the second variable τ. More precise technical assumptions on all these functions will be made later on.

2.1 The linear case

First, we focus on the linear case $r(u) = \lambda u$ where λ is a constant . In this case, we expand the initial data with respect to the periodic variable τ:

$$u_0(x) = \sum_{k \in \mathbb{Z}} f_k(x) e^{ik\beta(x)/\varepsilon},$$

which allows to restrict the study of (2.1) to the following equations

$$\partial_t u_k + c(x)\partial_x u_k + \lambda u_k = \frac{ia(x)}{\varepsilon} u_k, \quad u_k(t = 0, x) = f_k(x) e^{ik\beta(x)/\varepsilon}. \tag{2.2}$$

Indeed the linearity of the equation allows the use of the superposition principle, and the solution of (2.1) can be recovered by $u(t, x) = \sum_k u_k(t, x)$.

Since (2.2) is linear, one can apply the standard *Geometric Optics* (GO) by injecting the ansatz $u_k(t, x) = \alpha_k(t, x) e^{ikS(t,x)/\varepsilon}$ into (2.2). This gives

$$\partial_t \alpha_k + c(x)\partial_x \alpha_k + \lambda \alpha_k + \frac{i}{\varepsilon}[\partial_t S + c(x)\partial_x S]\alpha_k = \frac{ia(x)}{\varepsilon}\alpha_k.$$

To remove the terms in $1/\varepsilon$, one can impose the following equations on α and S

$$\partial_t \alpha_k + c(x)\partial_x \alpha_k + \lambda \alpha_k = 0, \quad \alpha(0, x) = f_k(x),$$
$$\partial_t S + c(x)\partial_x S = a(x), \quad S(0, x) = \beta(x).$$

This gives rise to *non oscillatory* solutions S and α_k which can be solved numerically quite efficiently without numerically resolving the small time and wavelength scales of size $O(\varepsilon)$.

2.2 The nonlinear case

When r is nonlinear, the superposition principle cannot be applied anymore and the GO approach does not work. Then, we utilize what was called in the literature the *nonlinear geometric optics* (NGO) ansatz, namely, introduce a function $U(t, x, \tau)$ which depends on an additional *periodic* variable τ, and satisfies

$$U(t, x, S(t, x)/\varepsilon) = u(t, x), \tag{2.3}$$

with u solution to (2.1). The equation satisfied by U writes

$$\partial_t U + c(x)\partial_x U + \frac{1}{\varepsilon}[\partial_t S + c(x)\partial_x S]\partial_\tau U + r(U) = \frac{ia(x)}{\varepsilon}U.$$

To get a constant period in the independent variable τ, we should impose the following equation on S

$$\partial_t S + c(x)\partial_x S = a(x), \quad S(0, x) = \beta(x). \tag{2.4}$$

Then, we deduce the equation for U to

$$\partial_t U + c(x)\partial_x U + r(U) = -\frac{a(x)}{\varepsilon}(\partial_\tau U - iU), \quad U(0, x, \beta(x)/\varepsilon) = u_0(x). \tag{2.5}$$

It is clear that solving (2.4) and (2.5) with any initial data $U(0, x, \tau)$ satisfying $U(0, x, \beta(x)/\varepsilon) = u_0(x)$ allows one to recover the desired original solution to (2.1) through relation (2.3). Due to the extra dimension introduced by U, there are infinitely many possible choices of such initial data. We will choose one–which is essential–that provides a "smooth enough" solution with respect to ε. Indeed, from numerical point of view, this smoothness property is of paramount importance when one wants to get a numerical scheme with a *uniform accuracy* with respect to ε. We will consider two cases for which this choice is possible and a uniform smoothness with respect to ε of the phase S and the profile U can be obtained at any order. The first case is very simple since the models on S and U do not depend on ε, while the second case requires more care and is presented in the next subsection.

Case 1: $a \equiv 0$ with possibly oscillatory initial data: $u_0(x) = f_{in}(x, \beta(x)/\varepsilon)$. The equation on the phase S is given by (2.4) and the equation on U reduces to

$$\partial_t U + c(x)\partial_x U + r(U) = 0, \qquad U(0, x, \tau) = f_{in}(x, \tau).$$

The two equations on S and U clearly do not depend on ε and therefore numerical schemes on S and U will not be restricted by the small values of ε.

Case 2: $a \neq 0$ with non-oscillatory initial data $u_0(x) = \alpha(x)$. In this case the equation for the phase S is still given by (2.4) with $\beta(x) = 0$, and the equation on U is also given by (2.5), which can be written in terms of

$$V = e^{-i\tau} U$$

where V solves

$$\partial_t V + c(x)\partial_x V + e^{-i\tau} r(e^{i\tau} V) = -\frac{a(x)}{\varepsilon}\partial_\tau V. \qquad (2.6)$$

Since the only condition one has to impose on V is $V(0, x, 0) = u_0(x)$ (recall that boundary conditions are imposed in x), this gives some freedom for the choice of the initial data for V, and the strategy of this choice will be developed in the next subsection.

Remark 2.1. *Our approach works with either oscillatory initial data, or oscillatory source. It does not apply to problems where oscillations are generated from both initially data and sources. See discussions in section 2.5.*

2.3 A suitable initial condition

Considering the non-oscillatory initial data (Case 2), one needs initial data $V(0, x, \tau)$ *for all* τ to solve equation (2.6) . Since the only condition we have to ensure is $V(0, x, 0) = u_0(x) = \alpha(x)$, there is a degree of freedom in choosing the expression of $V(0, x, \tau)$. *The central idea here is to choose it in such a way that the solution V is non-oscillatory in ε (up to certain order of time-space derivatives).* To show this construction, we will deal in this section with the case of non-oscillatory initial data, in which case we can construct $V(0, x, \tau)$

in such a way that the time-space derivatives of V (up to second order) are uniformly bounded with respect to ε.

Since the initial condition in (2.1) takes the non-oscillatory form $u(0,x) = \alpha(x)$, we have $S(0,x) = 0$. Following [7, 8], we will construct "well-prepared initial data" $V(0,x,\tau)$ which ensures that the high-order time and space derivatives of V are also bounded uniformly in ε, together with

$$V(0,x,\tau=0) = \alpha(x). \tag{2.7}$$

As a consequence, we will see that the so-obtained initial data for V provides a non-oscillatory solution V and allows the construction of numerical schemes with a uniform accuracy with respect to ε. Below, we will describe the method, and we refer to [7, 8] for more details. Note that this type of initial data is obtained by formally expanding the solution in terms of ε in the spirit of the well-known Chapman-Enskog expansion in kinetic theory [5]. For this purpose, we first introduce the notations

$$\mathcal{L}g = \partial_\tau g, \quad \Pi g = \frac{1}{2\pi}\int_0^{2\pi} g(\tau)d\tau,$$

and let

$$V^0 = \Pi V, \quad V^1 = (\mathcal{I} - \Pi)V.$$

The operator $\mathcal{L}$ is skew-symmetric on $L^2(d\tau)$, its kernel is the space of functions which do not depend on τ, and Π is the $L^2(d\tau)$-orthogonal projector onto the kernel of $\mathcal{L}$. The operator $\mathcal{L}$ is invertible on the set of functions having zero average in the variable τ, and

$$\mathcal{L}^{-1}g = (\mathcal{I} - \Pi)\int_0^\tau g(\sigma)d\sigma = \int_0^\tau g(\sigma)d\sigma + \frac{1}{2\pi}\int_0^{2\pi}\sigma g(\sigma)d\sigma,$$

for all $g \in L^2(d\tau)$ such that $\Pi g = 0$. In particular

$$\mathcal{L}^{-1}(e^{i\tau}) = -ie^{i\tau}, \qquad \mathcal{L}^{-1}(e^{-i\tau}) = ie^{-i\tau}.$$

In addition, $\mathcal{L}^{-1}$ is a bounded operator since $\|\mathcal{L}^{-1}g\|_{L_\tau^\infty} \leq C\|g\|_{L_\tau^\infty}$ and $\|\mathcal{L}^{-1}g\|_{L_\tau^2} \leq C\|g\|_{L_\tau^2}$ for all $g \in L^2(d\tau)$ such that $\Pi g = 0$.

We now apply Π and $\mathcal{I} - \Pi$ to (2.6) to get

$$\partial_t V^0 + c(x)\partial_x V^0 + \diamond[e^{-i\tau}r(e^{i\tau}(V^0 + V^1))] = 0, \tag{2.8}$$

$$\partial_t V^1 + c(x)\partial_x V^1 + (\mathcal{I} - \Pi)[e^{-i\tau}r(e^{i\tau}(V^0 + V^1))] = -\frac{a(x)}{\varepsilon}\partial_\tau V^1. \tag{2.9}$$

In particular (2.9) gives

$$V^1(t,x,\tau) = -\varepsilon(a(x))^{-1}\mathcal{L}^{-1}(\mathcal{I} - \Pi)[e^{-i\tau}r(e^{i\tau}V^0)] + O(\varepsilon^2), \tag{2.10}$$

which, when applied to (2.8) and letting $\varepsilon \to 0$, formally yields

$$\partial_t V^0 + c(x)\partial_x V^0 + \Pi[e^{-i\tau}r(e^{i\tau}(V^0))] = 0. \tag{2.11}$$

Then, one gets the following expansion for V

$$
\begin{aligned}
V(t,x,\tau) &= V^0(t,x) + V^1(t,x,\tau) \\
&= V^0(t,x) - \varepsilon(a(x))^{-1}\mathcal{L}^{-1}(\mathcal{I}-\Pi)[e^{-i\tau}r(e^{i\tau}V^0(t,x))] + O(\varepsilon^2). \ (2.12)
\end{aligned}
$$

To avoid oscillations in ε, this expansion should be satisfied at $t=0$ as well. Evaluating (2.12) at $t=\tau=0$ and using (2.7), this means that

$$
\alpha(x) = V^0(t=0,x) - \varepsilon(a(x))^{-1}\mathcal{L}^{-1}(\mathcal{I}-\Pi)[e^{-i\tau}r(e^{i\tau}V^0(t=0,x))]\Big|_{\tau=0} + O(\varepsilon^2),
$$

or

$$
V^0(t=0,x) = \alpha(x) + \varepsilon(a(x))^{-1}\mathcal{L}^{-1}(\mathcal{I}-\Pi)[e^{-i\tau}r(e^{i\tau}\alpha(x))]\Big|_{\tau=0} + O(\varepsilon^2). \quad (2.13)
$$

Evaluating (2.12) at $t=0$ and using (2.13) finally yields our suitable initial data:

$$
\begin{aligned}
V(0,x,\tau) &= \alpha(x) + \frac{\varepsilon}{a(x)}\Big[G(0,\alpha) - G(\tau,\alpha)\Big], \\
&\text{with} \quad G(\tau,\alpha) = \mathcal{L}^{-1}(\mathcal{I}-\Pi)[e^{-i\tau}r(e^{i\tau}\alpha(x))]. \quad (2.14)
\end{aligned}
$$

We will see that this approach not only allows one to capture the main oscillations with phase $S(t,x)$ and amplitude $O(1)$, it also allows to capture oscillations of amplitude ε.

Remark 2.2. *The Chapman-Enskog expansion is conducted only to generate the suitable initial data for V, while the equations for S and V (or U) are not asymptotically truncated. This guarantees that our method, unless other asymptotic methods, is accurate for all ε.*

Remark 2.3. *Another interest of the augmented formulation above is the following. Because of oscillations, in general the solution to (2.1) cannot converge strongly but only weakly when $\varepsilon \to 0$. However, if S is the solution to (2.4), then one may have (in some appropriate functional space)*

$$
\exp(-iS(t,x)/\varepsilon)u(t,x) = V(t,x,S(t,x)/\varepsilon) \quad \text{converges strongly to} \quad \bar{u} = \bar{u}(t,x)
$$

where $\bar{u}$ satisfies

$$
\partial_t\bar{u} + c(x)\partial_x\bar{u} + \Pi e^{-i\tau}r(e^{i\tau}\bar{u}) = 0, \qquad \bar{u}(0,x) = u_0(x). \quad (2.15)
$$

We will demonstrate this numerically in section 2.7. It will be interesting to investigate rigorously this strong convergence, but this task is beyond the scope of this paper and is deferred to a future work.

Now we will give a theorem which states that, up to the second order, time and space derivatives of V are bounded uniformly in ε, provided that the initial condition is given by (2.14). First, we make the following assumptions on r and a.

Assumption on r. We assume in the sequel that $r : \mathbb{R} \to \mathbb{R}$ is a twice differentiable function on $\mathbb{R}$ whose two first derivatives are bounded.

Assumption on a. $a : [0,1] \to \mathbb{R}$ is a $\mathcal{C}^2$ function satisfying $a(x) \geq a_0 > 0, \forall x \in [0,1]$.

Note that the assumption on a excludes the case of band crossing. There is no such a restriction for the actual numerical scheme, as will be demonstrated numerically later.

For the sake of simplicity, we will restrict ourselves in the following theorem to the case of a constant transport coefficient $c(x) = c > 0$. The extension to a non-constant $c(x)$ can easily be derived following the lines of the proof.

Theorem 2.4. *Let V be the solution of* (2.6) *on $[0,T]$. We consider the initial data* (2.14) *and periodic boundary condition in x and τ variables. Then, the time and spatial derivatives of V are bounded uniformly in $\varepsilon \in]0,1]$, that is, $\exists C > 0$ independent of ε such that $\forall t \in [0,T]$*

$$\|\partial_t^p V(t)\|_{L_{\tau,x}^\infty} \leq C, \quad and \quad \|\partial_x^p V(t)\|_{L_{\tau,x}^\infty} \leq C, \; for \; p = 0,1,2,$$

and

$$\|\partial_{xt}^2 V(t)\|_{L_{\tau,x}^\infty} \leq C, \quad and \quad \|\partial_\tau V(t)\|_{L_{\tau,x}^\infty} \leq C.$$

Proof of Theorem 2.4. First, we make the following change of variable

$$V(t,x,\tau) = W(S(t,x),x,\tau) \tag{2.16}$$

where S satisfies

$$\partial_t S + c\partial_x S = a(x), \qquad S(0,x) = 0.$$

In the one-dimensional case, one can write the exact solution for S

$$S(t,x) = \frac{1}{c}\Big[A(x) - A(x-ct)\Big], \quad \text{with } A(x) = \int_0^x a(y)dy. \tag{2.17}$$

Observe that, for all $x \in \mathbb{R}$, the phase $S(t,x)$ is an increasing function in t, and this property remains true in higher space dimensions. This means that the map $t \mapsto s = S(t,x)$ can be seen as a change of variable in time. Note that $s \in [0, \bar{T}]$, with $\bar{T} \leq (2/c)\|A\|_{L_x^\infty} \leq (2/c)\|a\|_{L_x^\infty}$. Then, $W(s,x,\tau)$ satisfies

$$\partial_s W + \frac{c}{a(x)}\partial_x W + \frac{1}{a(x)}e^{-i\tau}r(e^{i\tau}W) = -\frac{1}{\varepsilon}\partial_\tau W,$$

$$W(0,x,\tau) = V(0,x,\tau) = \alpha(x) + \frac{\varepsilon}{a(x)}\Big[G(0,\alpha) - G(\tau,\alpha)\Big],$$

$$\text{with } G(\tau,\alpha) = \mathcal{L}^{-1}(\mathcal{I} - \Pi)[e^{-i\tau}r(e^{i\tau}\alpha(x))]. \tag{2.18}$$

We then need to prove the following result for W.

Proposition 2.5. *Let W be the solution of* (2.18) *on* $[0, \bar{T}]$, *$\bar{T} > 0$, with periodic boundary condition in x and τ. Then, up to the second order, the time and spatial derivatives of W are bounded uniformly in $\varepsilon \in]0, 1]$, that is, $\exists C > 0$ independent of ε such that, $\forall s \in [0, \bar{T}]$*

$$\|\partial_s^p W(s)\|_{L_{\tau,x}^\infty} \leq C, \quad and \quad \|\partial_x^p W(s)\|_{L_{\tau,x}^\infty} \leq C, \ for \ p = 0, 1, 2,$$

and

$$\|\partial_{st}^2 W(s)\|_{L_{\tau,x}^\infty} \leq C.$$

We first claim that this proposition implies the result of Theorem 2.4. Indeed, using the following straightforward relations

$$
\begin{aligned}
\partial_t V &= \partial_s W \partial_t S, \\
\partial_t^2 V &= \partial_s^2 W (\partial_t S)^2 + \partial_s W \partial_t^2 S, \\
\partial_x V &= \partial_s W \partial_x S + \partial_x W, \\
\partial_x^2 V &= \partial_s^2 W (\partial_x S)^2 + \partial_s W \partial_x^2 S + \partial_{xs}^2 W (\partial_x S) + \partial_x^2 W, \\
\partial_{tx}^2 V &= \partial_s^2 W (\partial_t S)(\partial_x S) + \partial_s W \partial_{tx}^2 S + \partial_{sx}^2 W \partial_t S,
\end{aligned}
$$

and the fact that $S(t, x)$ given by (2.17) has its time and space derivatives uniformly bounded (since S does not depend on ε), the estimates stated in Theorem 2.4 hold. □

Now, we focus on the proof of Proposition 2.5. To this aim, we start with the following elementary lemma:

Lemma 2.6. *Consider the following ordinary differential equation*

$$\frac{dy^\varepsilon}{dt} = \alpha^\varepsilon(t) y^\varepsilon + \beta^\varepsilon(t), \ \ t \in [0, T], \ \ y^\varepsilon(0) = y_0^\varepsilon,$$

with $y^\varepsilon, \alpha^\varepsilon, \beta^\varepsilon : [0, T] \to \mathcal{H}$, $\mathcal{H}$ being a Banach algebra space. Assume that there exists a constant $C > 0$ independent of ε such that $\|\alpha^\varepsilon(t)\|_{\mathcal{H}} \leq C$ and $\|\beta^\varepsilon(t)\|_{\mathcal{H}} \leq C$, $\forall t \in [0, T]$. Then there exists a constant $M > 0$ independent of ε such that $\|y^\varepsilon(t)\|_{\mathcal{H}} \leq M \|y_0^\varepsilon\|_{\mathcal{H}}$, $\forall t \leq T$.

Proof of Lemma 2.6. The proof of Lemma 2.6 follows from the exact solution which can be written as

$$y^\varepsilon(t) = y_0^\varepsilon \exp\left(\int_0^t \alpha^\varepsilon(s) ds\right) + \int_0^t \left[\exp\left(\int_s^t \alpha^\varepsilon(u) du\right) \beta^\varepsilon(s)\right] ds.$$

Then, one can straightforwardly deduce from the assumptions on α and β, that $\forall t \in [0, T]$, $\|y^\varepsilon(t)\|_{\mathcal{H}} \leq M \|y_0^\varepsilon\|_{\mathcal{H}}$.

□

In the following, we will use this lemma to prove that the time and space derivatives of W, solution of (2.18), are uniformly bounded in the space $\mathcal{H} = L_{\tau,x}^\infty$ of bounded functions of τ and x.

Proof of Proposition 2.5. We first introduce the characteristic equations associated with (2.18),

$$\dot{x}(s) = \frac{c}{a(x(s))}, \quad x(0) = x_0; \quad \dot{\tau}(s) = \frac{1}{\varepsilon}, \quad \tau(0) = \tau_0.$$

Since c is a constant, this system can be solved analytically. For A given by (2.17), since $a > 0$, A is a strictly increasing function, thus its inverse A^{-1} is well defined so that the solution of the differential system is

$$x(s) = A^{-1}(A(x_0) + cs), \quad x(0) = x_0; \quad \tau(s) = \tau_0 + \frac{s}{\varepsilon}, \quad \tau(0) = \tau_0.$$

This motivates the following change of variables

$$\tilde{x} = A^{-1}(A(x) + cs), \quad \tilde{\tau} = \tau + \frac{s}{\varepsilon}, \tag{2.19}$$

which enables to filter out the transport terms in (2.18).

Existence and estimate of W

Using (2.19), we write the equation satisfied by $\widetilde{W}(s, x, \tau) = W(s, A^{-1}(A(x) + cs), \tau + \frac{s}{\varepsilon})$ to get

$$\partial_s \widetilde{W} = -\frac{1}{a(\tilde{x})} e^{-i\tilde{\tau}} r(e^{i\tilde{\tau}} \widetilde{W}), \tag{2.20}$$

where $\tilde{x}$ and $\tilde{\tau}$ are given by (2.19), and with the initial condition $\widetilde{W}(0, x, \tau) = V(0, x, \tau)$ given by (2.18). Since r is a Lipschitz function, according to the Cauchy-Lipschitz theorem in the Banach space $L^\infty_{\tau,x}$, equation (2.20) has a unique global solution. Furthermore, since $a(\tilde{x}) \geq a_0 > 0$, we have

$$
\begin{aligned}
\|\widetilde{W}(s)\|_{L^\infty_{\tau,x}} &\leq \|V(0)\|_{L^\infty_{\tau,x}} + C \left\| \int_0^s \frac{1}{a(\tilde{x})} e^{-i\tilde{\tau}} r(e^{i\tilde{\tau}} \widetilde{W}(\sigma)) d\sigma \right\|_{L^\infty_{\tau,x}} \\
&\leq \|V(0)\|_{L^\infty_{\tau,x}} + C \int_0^s (1 + \|\widetilde{W}(\sigma)\|_{L^\infty_{\tau,x}}) d\sigma,
\end{aligned}
$$

and using the Gronwall lemma, we get

$$\sup_{\varepsilon > 0} \|\widetilde{W}(s)\|_{L^\infty_{\tau,x}} \leq C(1 + \|V(0)\|_{L^\infty_{\tau,x}}). \tag{2.21}$$

Since the initial data $V(0)$, given by (2.14), is uniformly bounded with respect to ε, we deduce that $\widetilde{W}$, and then W, are also uniformly bounded.

We now prove that time and space derivatives, up to the second order, are bounded uniformly in ε.

Estimate of the first time derivative

The first derivative $W_1 = \partial_s W$ satisfies

$$\partial_s W_1 + \frac{c}{a(x)} \partial_x W_1 + \frac{1}{a(x)} r'(e^{i\tau} W) W_1 = -\frac{1}{\varepsilon} \partial_\tau W_1. \tag{2.22}$$

11

As before, we consider the change of variables (2.19) so that $\widetilde{W}_1(s, x, \tau) = W_1(s, A^{-1}(A(x) + cs), \tau + \frac{s}{\varepsilon})$ solves

$$\partial_s \widetilde{W}_1 + \frac{1}{a(\tilde{x})} r'(e^{i\tilde{\tau}} \widetilde{W}) \widetilde{W}_1 = 0.$$

This equation enters in the framework of Lemma 2.6 with $\alpha^\varepsilon(s) = (1/a(\tilde{x})) r'(e^{i\tilde{\tau}} \widetilde{W}(s))$ and $\beta^\varepsilon(s) = 0$. Under the assumption on r and the estimate (2.21) on $\widetilde{W}$, $\widetilde{W}_1(s)$ is uniformly bounded provided that $\widetilde{W}_1(0)$ is bounded. From equation (2.18) on W at $s = 0$, one has

$$
\begin{aligned}
\widetilde{W}_1(0) &= \partial_s W(0) \\
&= -\frac{1}{\varepsilon} \partial_\tau W(0) - \frac{c}{a(x)} \partial_x W(0) - \frac{1}{a(x)} e^{-i\tau} r(e^{i\tau} W(0)).
\end{aligned}
$$

The last term is bounded using the assumption on r and the fact that $W(0)$ is bounded. Considering the first term, with the choice of $W(0)$ given by (2.18), one gets

$$
\begin{aligned}
\left| \frac{1}{\varepsilon} \partial_\tau W(0) \right| &= \left| \frac{1}{a(x)} (I - \Pi)(e^{-i\tau} r(e^{i\tau} \alpha(x))) \right| \\
&\leq C \| r(e^{i\tau} \alpha) \|_{L^\infty_{x,\tau}} \leq C(1 + \|\alpha\|_{L^\infty_x}).
\end{aligned}
$$

Then, for the second term, using the notations in (2.18),

$$
\begin{aligned}
\partial_x W(0) &= \alpha'(x) - \frac{\varepsilon a'(x)}{a(x)^2} \Big[G(0, \alpha) - G(\tau, \alpha) \Big] \\
&\quad + \frac{\varepsilon}{a(x)} \Big[H(0, \alpha) - H(\tau, \alpha) \Big],
\end{aligned}
\tag{2.23}
$$

where $H(\tau, \alpha) =: \partial_x G(\tau, \alpha) = \mathcal{L}^{-1}(\mathcal{I} - \Pi)(r'(e^{i\tau} \alpha(x)) \alpha'(x))$. Using the fact that $\mathcal{L}^{-1}$ is a bounded operator on $\mathcal{C}^0(\mathbb{T})$ and the assumptions on r, we get $\|G\|_{L^\infty_{x,\tau}} \leq C(1 + \|\alpha\|_{L^\infty_x})$ and $\|H\|_{L^\infty_{x,\tau}} \leq C(1 + \|\alpha\|_{L^\infty_x}) \|\alpha'\|_{L^\infty_x}$. Finally, we have

$$
\begin{aligned}
\left| \partial_x W(0) \right| &\leq |\alpha'(x)| + C \left| \frac{\varepsilon a'(x)}{a(x)^2} \right| (1 + \|\alpha\|_{L^\infty_x}) + \frac{\varepsilon}{a} \|\alpha'\|_{L^\infty_x} \\
&\leq \frac{C\varepsilon}{a_0^2} + \|\alpha\|_{W_x^{1,\infty}} \left[1 + C \frac{\varepsilon}{a_0^2} + C \frac{\varepsilon}{a_0} \right] \leq C.
\end{aligned}
\tag{2.24}
$$

We then conclude that $\widetilde{W}_1(0) = \partial_s W(0)$ is uniformly bounded. As a consequence,

$$\|\widetilde{W}_1(s)\|_{L^\infty_{\tau,x}} \leq C, \tag{2.25}$$

and then $\partial_s W$ is uniformly bounded in ε.

Estimate of the second time derivative

We proceed in a analogous way for $W_2 = \partial_s^2 W = \partial_s W_1$ by taking the time derivative of equation (2.22), which satisfies

$$\partial_s W_2 + \frac{c}{a(x)}\partial_x W_2 + \frac{1}{a(x)}e^{i\tau}r''(e^{i\tau}W)W_1^2 + \frac{1}{a(x)}r'(e^{i\tau}W)W_2 = -\frac{1}{\varepsilon}\partial_\tau W_2.$$
(2.26)

Using (2.19), $\widetilde{W}_2(t,x,\tau) = W_2(s, A^{-1}(A(x)+cs), \tau + \frac{s}{\varepsilon})$ satisfies

$$\partial_s \widetilde{W}_2 + \frac{1}{a(\tilde{x})}r'(e^{i\tilde{\tau}}\widetilde{W})\widetilde{W}_2 + \frac{1}{a(\tilde{x})}e^{i\tilde{\tau}}r''(e^{i\tilde{\tau}}\widetilde{W})\widetilde{W}_1^2 = 0.$$

We now use Lemma 2.6 with $\alpha^\varepsilon(s) = (1/a(\tilde{x}))r'(e^{i\tilde{\tau}}\widetilde{W})$ and $\beta^\varepsilon(s) = (1/a(\tilde{x}))e^{i\tilde{\tau}}r''(e^{i\tilde{\tau}}\widetilde{W})\widetilde{W}_1^2$. Using (2.21), (2.25) and the assumption on r, one deduces that $\alpha^\varepsilon(s)$ and $\beta^\varepsilon(s)$ are uniformly bounded, and one just needs to prove that the initial data $\widetilde{W}_2(0) = W_2(0)$ is bounded uniformly in ε. Let us recall the expression of $W_2(0)$ using (2.22) at $s = 0$

$$W_2(0) = \partial_s W_1(0) = -\frac{c}{a(x)}\partial_x W_1(0) - \frac{1}{a(x)}r'(e^{i\tau}W(0))W_1(0) - \frac{1}{\varepsilon}\partial_\tau W_1(0).$$
(2.27)

The second term in the right hand side is uniformly bounded since W and W_1 are bounded. The terms $\frac{1}{\varepsilon}\partial_\tau W_1(0)$ and $\frac{c}{a(x)}\partial_x W_1(0)$ need more care. First we write $W_1(0)$ using (2.18)

$$
\begin{aligned}
W_1(0) &= \partial_s W(0) = -\frac{c}{a(x)}\partial_x W(0) - \frac{1}{a(x)}e^{-i\tau}r(e^{i\tau}W(0)) - \frac{1}{\varepsilon}\partial_\tau W(0) \\
&= -\frac{c}{a(x)}\partial_x W(0) - \frac{1}{a(x)}e^{-i\tau}r(e^{i\tau}W(0)) + \frac{1}{a(x)}(\mathcal{I}-\Pi)[e^{-i\tau}r(e^{i\tau}\alpha(x))] \\
&= -\frac{c}{a(x)}\partial_x W(0) + \frac{1}{a(x)}e^{-i\tau}[r(e^{i\tau}\alpha(x)) - r(e^{i\tau}W(0))] \\
&\quad -\frac{1}{a(x)}\Pi[e^{-i\tau}r(e^{i\tau}\alpha(x))].
\end{aligned}
$$
(2.28)

Then, we compute $(1/\varepsilon)\partial_\tau W_1(0)$ using (2.18)

$$
\begin{aligned}
\frac{1}{\varepsilon}\partial_\tau W_1(0) &= -\frac{c}{a\varepsilon}\partial_{\tau x}^2 W(0) + \frac{1}{a\varepsilon}\partial_\tau\Big[e^{-i\tau}[r(e^{i\tau}\alpha) - r(e^{i\tau}W(0))]\Big] \\
&= -\frac{c}{a\varepsilon}\Big[\frac{\varepsilon a'}{a^2}(\mathcal{I}-\Pi)[e^{-i\tau}r(e^{i\tau}\alpha)] - \frac{\varepsilon}{a}(\mathcal{I}-\Pi)[\alpha'r'(e^{i\tau}\alpha)]\Big] \\
&\quad +\frac{1}{a\varepsilon}\big\{-ie^{-i\tau}[r(e^{i\tau}\alpha) - r(e^{i\tau}W(0))] + i\alpha r'(e^{i\tau}\alpha) \\
&\quad -r'(e^{i\tau}W(0))[iW(0) + \partial_\tau W(0)]\big\} \\
&= -\frac{ca'}{a^3}(\mathcal{I}-\Pi)[e^{-i\tau}r(e^{i\tau}\alpha)] + \frac{c}{a^2}(\mathcal{I}-\Pi)[\alpha'r'(e^{i\tau}\alpha)] \\
&\quad -\frac{i}{a\varepsilon}e^{-i\tau}[r(e^{i\tau}\alpha) - r(e^{i\tau}W(0))] + \frac{1}{a\varepsilon}r'(e^{i\tau}W(0))\frac{\varepsilon}{a}(\mathcal{I}-\Pi)[e^{-i\tau}r(e^{i\tau}\alpha)] \\
&\quad +\frac{i}{a\varepsilon}\Big[r'(e^{i\tau}\alpha)\alpha - r'(e^{i\tau}W(0))W(0)\Big].
\end{aligned}
$$

Using the fact that $\mathcal{L}^{-1}$ is a bounded operator on $\mathcal{C}^0(\mathbb{T})$ and the smoothness assumptions on r, one gets

$$\left|\frac{1}{\varepsilon}\partial_\tau W_1(0)\right| \leq \frac{C}{a_0^3}(1+|\alpha|) + \frac{C}{a_0^2} + \frac{1}{a_0\varepsilon}C|\alpha - W(0)| + \frac{C}{a_0^2}(1+|\alpha|) + \frac{1}{a_0\varepsilon}C|\alpha - W(0)|.$$

From (2.18), since $W(0) - \alpha = \frac{\varepsilon}{a}[G(0, \alpha) - G(\tau, \alpha)]$ with G uniformly bounded, one has

$$\left|\frac{1}{\varepsilon}\partial_\tau W_1(0)\right| \leq C.$$

We now focus on the term $\partial_x W_1(0)$ (which is the first term in the rhs of (2.27)) and take the derivative of (2.28) with respect to x

$$\begin{aligned}
\partial_x W_1(0) &= \frac{ca'}{a^2}\partial_x W(0) - \frac{c}{a}\partial_x^2 W(0) - \frac{a'}{a^2}e^{-i\tau}[r(e^{i\tau}\alpha) - r(e^{i\tau}W(0))] \\
&\quad + \frac{1}{a}[\alpha' r'(e^{i\tau}\alpha) - \partial_x W(0)r'(e^{i\tau}W(0))] \\
&\quad + \frac{a'}{a^2}\Pi[e^{-i\tau}r(e^{i\tau}\alpha)] - \frac{1}{a}\Pi[\alpha' r'(e^{i\tau}\alpha)].
\end{aligned} \tag{2.29}$$

All the terms except the first one $\partial_x^2 W(0)$ have been estimated previously. Express $\partial_x^2 W(0)$ by taking the derivative of (2.23) with respect to x

$$\begin{aligned}
\partial_x^2 W(0) &= \alpha'' - \varepsilon\frac{a''a - 2(a')^2}{a^3}[G(\tau = 0, \alpha) - G(\tau, \alpha)] \\
&\quad - 2\frac{\varepsilon a'}{a^2}\partial_x[G(\tau = 0, \alpha) - G(\tau, \alpha)] + \frac{\varepsilon}{a}\partial_x^2[G(\tau = 0, \alpha) - G(\tau, \alpha)],
\end{aligned}$$

where $G(\tau, \alpha) = \mathcal{L}^{-1}(\mathcal{I} - \Pi)(e^{-i\tau}r(e^{i\tau}\alpha(x)))$ is used. Using the properties of $\mathcal{L}^{-1}$ and of r and a, one can estimate $\partial_x^2 W(0)$

$$\begin{aligned}
|\partial_x^2 W(0)| &\leq \|\alpha''\|_{L_x^\infty} + \frac{C\varepsilon}{a_0^3}(1 + \|\alpha\|_{L_x^\infty}) + \frac{C\varepsilon}{a_0^2}\|\alpha'\|_{L_x^\infty} + \frac{\varepsilon}{a_0}\|\alpha''\|_{L_x^\infty} \\
&\leq C.
\end{aligned} \tag{2.30}$$

Thus, from (2.27), $W_2(0)$ is uniformly bounded and we conclude with Lemma 2.6 that

$$\|\widetilde{W_2}(s)\|_{L_{\tau,x}^\infty} \leq C, \tag{2.31}$$

so that $\partial_s^2 W$ is uniformly bounded.

First space derivative

The function $Y_1 = \partial_x W$ solves the following equation

$$\partial_s Y_1 + \frac{c}{a}\partial_x Y_1 - \frac{ca'}{a^2}Y_1 - \frac{a'}{a^2}e^{-i\tau}r(e^{i\tau}W) + \frac{1}{a}r'(e^{i\tau}W)Y_1 = -\frac{1}{\varepsilon}\partial_\tau Y_1. \tag{2.32}$$

14

Again the function $\widetilde{Y}_1(t,x,\tau) = Y_1(s, A^{-1}(A(x) + cs), \tau + \frac{s}{\varepsilon})$ satisfies

$$\partial_s \widetilde{Y}_1 - \frac{ca'(\tilde{x})}{a(\tilde{x})^2}\widetilde{Y}_1 - \frac{a'(\tilde{x})}{a(\tilde{x})^2}e^{-i\tilde{\tau}}r(e^{i\tilde{\tau}}\widetilde{W}) + \frac{1}{a(\tilde{x})}r'(e^{i\tilde{\tau}}\widetilde{W})\widetilde{Y}_1 = 0,$$

where we used the notation in (2.19). Then, one can use Lemma 2.6 with $\alpha^\varepsilon(s) = -(1/a(\tilde{x}))r'(e^{i\tilde{\tau}}\widetilde{W}) + (ca'(\tilde{x})/a(\tilde{x})^2)$ and $\beta^\varepsilon(s) = (a'(\tilde{x})/a(\tilde{x})^2)e^{-i\tilde{\tau}}r(e^{i\tilde{\tau}}\widetilde{W})$ for which one gets a uniform estimate thanks to the assumption on r and the previous estimate on $\widetilde{W}$. Moreover, it has already been proved in (2.24) that the initial condition $\widetilde{Y}_1(0) = \partial_x W(0)$ (with $W(0)$ given by (2.14)) is uniformly bounded. As a consequence,

$$\|\widetilde{Y}_1(s)\|_{L^\infty_{\tau,x}} \leq C. \tag{2.33}$$

so that $Y_1(s) = \partial_x W(s)$ is also uniformly bounded with repsect to ε.

Second space derivative

Considering $Y_2 = \partial_x^2 W = \partial_x Y_1$, one gets from (2.32)

$$\partial_s Y_2 + \frac{c}{a}\partial_x Y_2 - \frac{2ca'}{a^2}Y_2 - c\frac{a''a - 2(a')^2}{a^3}Y_1 - \frac{2a'}{a^2}r'(e^{i\tau}W)Y_1 + \frac{1}{a}e^{i\tau}r''(e^{i\tau}W)Y_1^2$$

$$+\frac{1}{a}r'(e^{i\tau}W)Y_2 - \frac{a''a - 2(a')^2}{a^3}e^{-i\tau}r(e^{i\tau}W) = -\frac{1}{\varepsilon}\partial_\tau Y_2. \tag{2.34}$$

Again, with the change of variable (2.19), the equation for $\widetilde{Y}_2(s,x,\tau) = Y_2(t, x + ct, \frac{1}{c\varepsilon}[A(x+ct) - A(x)] + \tau)$ writes (using the notations introduced above)

$$\partial_t \widetilde{Y}_2 = \alpha^\varepsilon(s)\widetilde{Y}_2 + \beta^\varepsilon(s),$$

where

$$\alpha^\varepsilon(s) = \frac{2ca'(\tilde{x})}{a(\tilde{x})^2} - \frac{1}{a(\tilde{x})}r'(e^{i\tilde{\tau}}\widetilde{W})$$

$$\beta^\varepsilon(s) = c\frac{a''(\tilde{x})a(\tilde{x}) - 2(a'(\tilde{x}))^2}{a(\tilde{x})^3}\widetilde{Y}_1 + \frac{2a'(\tilde{x})}{a(\tilde{x})^2}r'(e^{i\tilde{\tau}}\widetilde{W})\widetilde{Y}_1 - \frac{1}{a(\tilde{x})}e^{i\tilde{\tau}}r''(e^{i\tilde{\tau}}\widetilde{W})\widetilde{Y}_1^2$$

$$+\frac{a''(\tilde{x})a(\tilde{x}) - 2(a'(\tilde{x}))^2}{a(\tilde{x})^3}e^{-i\tilde{\tau}}r(e^{i\tilde{\tau}}\widetilde{W}),$$

are uniformly bounded thanks to the previous estimates and the properties of r. One then needs to check that the initial condition $\widetilde{Y}_2(0) = Y_2(0) = \partial_x^2 W(0)$ is uniformly bounded, but we recall that $\partial_x^2 W(0)$ has already been estimated in (2.30). Hence, we can conclude

$$\|\widetilde{Y}_2(s)\|_{L^\infty_{\tau,x}} \leq C, \tag{2.35}$$

so that Y_2 is uniformly bounded with respect to ε.

Mixed space-time derivative

By differentiating (2.32) with respect to s, one gets the equation satisfied by $Y_3 = \partial_s Y_1 = \partial_{sx}^2 W$

$$\partial_t Y_3 + \frac{c}{a}\partial_x Y_3 - \frac{ca'}{a^2}Y_3 - \frac{a'}{a^2}r'(e^{i\tau}W)W_1 + \frac{1}{a}e^{i\tau}r''(e^{i\tau}W)W_1 Y_1 + \frac{1}{a}r'(e^{i\tau}W)Y_3 = -\frac{1}{\varepsilon}\partial_\tau Y_3.$$
(2.36)

Using (2.19), $\widetilde{Y}_3(t,x,\tau) = Y_3(s, A^{-1}(A(x)+cs), \tau + \frac{s}{\varepsilon})$ satisfies

$$\partial_t \widetilde{Y}_3 - \frac{ca'(\tilde{x})}{a(\tilde{x})^2}\widetilde{Y}_3 - \frac{a'(\tilde{x})}{a(\tilde{x})^2}r'(e^{i\tilde{\tau}}\widetilde{W})\widetilde{W}_1 + \frac{1}{a(\tilde{x})}e^{i\tilde{\tau}}r''(e^{i\tilde{\tau}}\widetilde{W})\widetilde{W}_1\widetilde{Y}_1 + \frac{1}{a(\tilde{x})}r'(e^{i\tilde{\tau}}\widetilde{W})\widetilde{Y}_3 = 0.$$
(2.37)

We use Lemma 2.6 with $\alpha^\varepsilon(s) = (ca'(\tilde{x})/a(\tilde{x})^2) - (1/a(\tilde{x}))r'(e^{i\tilde{\tau}}\widetilde{W})$ and $\beta^\varepsilon(s) = (a'(\tilde{x})/a(\tilde{x})^2)r'(e^{i\tilde{\tau}}\widetilde{W})\widetilde{W}_1 - (1/a(\tilde{x}))e^{i\tilde{\tau}}r''(e^{i\tilde{\tau}}\widetilde{W})\widetilde{W}_1\widetilde{Y}_1$ which are uniformly bounded thanks to the previous estimates and the smoothness of r. One now needs to check that the initial condition $\partial_{sx}W(0)$ is uniformly bounded. To do so, apply (2.32) at $s = 0$ to get

$$
\begin{aligned}
\partial_{sx}^2 W(0) &= -\frac{c}{a}\partial_x Y_1(0) + \frac{ca'}{a^2}Y_1(0) + \frac{a'}{a^2}e^{-i\tau}r(e^{i\tau}W(0)) - \frac{1}{a}r'(e^{i\tau}W(0))Y_1(0) - \frac{1}{\varepsilon}\partial_\tau Y_1(0) \\
&= -\frac{c}{a}\partial_x^2 W(0) + \frac{ca'}{a^2}\partial_x W(0) + \frac{a'}{a^2}e^{-i\tau}r(e^{i\tau}W(0)) \\
&\quad -\frac{1}{a}r'(e^{i\tau}W(0))\partial_x W(0) - \frac{1}{\varepsilon}\partial_{x\tau}W(0)
\end{aligned}
$$
(2.38)

All the terms except the last one have already been estimated previously. Let us focus on $\frac{1}{\varepsilon}\partial_{x\tau}^2 W(0)$

$$
\begin{aligned}
\left|\frac{1}{\varepsilon}\partial_{x\tau}^2 W(0)\right| &= \left|-\frac{1}{\varepsilon}\partial_x\left[\frac{\varepsilon}{a}(\mathcal{I}-\Pi)[e^{-i\tau}r(e^{i\tau}\alpha)]\right]\right| \\
&= \left|\frac{a'}{a^2}(\mathcal{I}-\Pi)[e^{-i\tau}r(e^{i\tau}\alpha)] - \frac{1}{a}(\mathcal{I}-\Pi)[r'(e^{i\tau}\alpha)\alpha']\right| \\
&\leq \frac{|a'|}{a_0^2}(1 + \|\alpha\|_{L_x^\infty}) + \frac{C}{a_0}\|\alpha'\|_{L_x^\infty},
\end{aligned}
$$

which is uniformly bounded. Then, we conclude that

$$\|\widetilde{Y}_3(t)\|_{L_{\tau,x}^\infty} \leq C,$$
(2.39)

so that $\partial_{sx}^2 W$ is bounded uniformly with respect to ε.

$\square$

2.4   A numerical scheme for the equation of V

In this section, we focus on the numerical analysis of a first order (in time and space) numerical scheme for the equation of V: (2.6), with initial condition

(2.14), in which the variable τ is kept continuous. For the sake of simplicity, our convergence analysis will be restricted to constant and nonnegative convection term $c(x) = c$. We also assume that $a(x) \geq a_0$ for all $x \in [0,1]$, where a_0 is a positive constant. The numerical tests, however, will not be restricted by these assumptions.

We define a uniform grid in time $t_n = n\Delta t$ in a time interval $[0,T]$, $n = 0,1,\ldots,N$, $N\Delta t = T$ and in space $x_j = j\Delta x$, $j = 0,1,\ldots,N_x$, $\Delta x = 1/N_x$ in the spatial interval $[0,1]$ (recall that periodic boundary conditions are considered in space). Denoting $V_j^n(\tau) \approx V(t_n, x_j, \tau)$, $\tau \in \mathbb{T} = [0, 2\pi]$, the numerical scheme for (2.6) advances the solution from t_n to t_{n+1} through

$$\frac{V_j^{n+1} - V_j^n}{\Delta t} + c\frac{V_j^n - V_{j-1}^n}{\Delta x} + e^{-i\tau}r(e^{i\tau}V_j^n) = -\frac{a(x_j)}{\varepsilon}\partial_\tau V_j^{n+1}, \qquad (2.40)$$

with $V_j^0(\tau)$ given by (2.14). In this scheme, the spatial discretization is the upwind scheme. In the following theorem, we prove that the numerical scheme (2.40), with initial data (2.14), is not only a first order approximation of (2.6), but more importantly this first order approximation is *uniform* in ε.

Theorem 2.7. *Assume that $a : [0,1] \to \mathbb{R}$ is a $\mathcal{C}^2$ function satisfying $a(x) \geq a_0 > 0, \forall x \in [0,1]$, and that the CFL condition $c\Delta t/\Delta x < 1$ is satisfied. Then $\exists C > 0$ independent of $\Delta t, \Delta x$ and ε, such that*

$$\sup_{\varepsilon \in]0,1]} \|V(t_n, x_j) - V_j^n\|_{L_\tau^\infty} \leq C(\Delta t + \Delta x), \qquad (2.41)$$

for all $n = 0,\ldots,N$, $n\Delta t \leq T$ and all $j = 0,\ldots,N_x$.

Proof. First, we check that the scheme is well defined. Assuming V_j^n is periodic in τ with period 2π, then it is easy to see that V_j^{n+1} is also periodic with period 2π. We proceed in an analogous way as in [7] and introduce the operator Q_j defined from $\mathcal{C}^1(\mathbb{T})$ into $\mathcal{C}^0(\mathbb{T})$ by

$$\forall \tau \in \mathbb{T}, \ \ (Q_j g)(\tau) = g(\tau) + \frac{a(x_j)}{\varepsilon}(\partial_\tau g)(\tau). \qquad (2.42)$$

This operator is invertible and its inverse can be written as

$$\forall \tau \in \mathbb{T}, \ \ (Q_j^{-1}g)(\tau) = \frac{\varepsilon/a(x_j)}{\exp(\varepsilon/a(x_j)2\pi) - 1}\int_\tau^{\tau+2\pi} \exp(\varepsilon/a(x_j)(\theta - \tau))g(\theta)d\theta.$$

Moreover, since

$$\frac{\varepsilon/a(x_j)}{\exp(\varepsilon/a(x_j)2\pi) - 1}\int_0^{2\pi} \exp(\varepsilon/a(x_j)\theta)d\theta = 1,$$

one gets

$$\forall g \in \mathcal{C}^0(\mathbb{T}), \ \ \|Q_j^{-1}g\|_{L_\tau^\infty} \leq \|g\|_{L_\tau^\infty}, \ \ \forall j = 0, \cdots, N_x. \qquad (2.43)$$

Let us now study the error of the scheme (2.40). First, we perform Taylor expansions in time and space. On the one side, one gets

$$
\frac{V(t_{n+1}, x_j) - V(t_n, x_j)}{\Delta t}
$$

$$
= \partial_t V(t_{n+1}, x_j) - \frac{1}{\Delta t} \int_{t_n}^{t_{n+1}} (t - t_n) \partial_t^2 V(t, x_j) dt
$$

$$
= -c \partial_x V(t_{n+1}, x_j) - e^{-i\tau} r(e^{i\tau} V(t_{n+1}, x_j)) - \frac{a(x_j)}{\varepsilon} \partial_\tau V(t_{n+1}, x_j)
$$

$$
- \frac{1}{\Delta t} \int_{t_n}^{t_{n+1}} (t - t_n) \partial_t^2 V(t, x_j) dt.
$$

And on the other side,

$$
\frac{V(t_n, x_j) - V(t_n, x_{j-1})}{\Delta x} = \partial_x V(t_n, x_j) - \frac{1}{\Delta x} \int_{x_{j-1}}^{x_j} (x - x_{j-1}) \partial_x^2 V(t_n, x) dx.
$$

Gathering both equalities gives

$$
\frac{V(t_{n+1}, x_j) - V(t_n, x_j)}{\Delta t} + c \frac{V(t_n, x_j) - V(t_n, x_{j-1})}{\Delta x}
$$

$$
= -c \partial_x V(t_{n+1}, x_j) - e^{-i\tau} r(e^{i\tau} V(t_{n+1}, x_j)) + (R_t)_j^n
$$

$$
- \frac{a(x_j)}{\varepsilon} \partial_\tau V(t_{n+1}, x_j) + c \partial_x V(t_n, x_j) + (R_x)_j^n,
$$

$$
= -c \partial_x [V(t_{n+1}, x_j) - V(t_n, x_j)] + (R_t)_j^n + (R_x)_j^n
$$

$$
- e^{-i\tau} r(e^{i\tau} V(t_{n+1}, x_j)) - \frac{a(x_j)}{\varepsilon} \partial_\tau V(t_{n+1}, x_j)
$$

$$
= -c \int_{t_n}^{t_{n+1}} \partial_{xt}^2 V(t, x_j) dt + (R_t)_j^n + (R_x)_j^n
$$

$$
- e^{-i\tau} r(e^{i\tau} V(t_{n+1}, x_j)) - \frac{a(x_j)}{\varepsilon} \partial_\tau V(t_{n+1}, x_j), \qquad (2.44)
$$

where $(R_x)_j^n = -\frac{c}{\Delta x} \int_{x_{j-1}}^{x_j} (x - x_{j-1}) \partial_x^2 V(t_n, x) dx$ and $(R_t)_j^n = -\frac{1}{\Delta t} \int_{t_n}^{t_{n+1}} (t - t_n) \partial_t^2 V(t, x_j) dt$ denote the integral remainders of the previous Taylor expansions.

Denoting by $\mathcal{E}_j^n = V(t_n, x_j) - V_j^n$ the error, the difference between (2.44) and (2.40) gives

$$
\frac{\mathcal{E}_j^{n+1} - \mathcal{E}_j^n}{\Delta t} + c \frac{\mathcal{E}_j^n - \mathcal{E}_{j-1}^n}{\Delta x} + e^{-i\tau} \left[r(e^{i\tau} V(t_{n+1}, x_j)) - r(e^{i\tau} V_j^n) \right] + c \int_{t_n}^{t_{n+1}} \partial_{xt}^2 V(t, x_j) dt
$$

$$
= (R_x)_j^n + (R_t)_j^n - \frac{a(x_j)}{\varepsilon} \partial_\tau \mathcal{E}_j^{n+1}. \qquad (2.45)
$$

18

Here, we focus on the third term of the left hand side of (2.45)

$$e^{-i\tau}\Big[r(e^{i\tau}V(t_{n+1},x_j)) - r(e^{i\tau}V_j^n)\Big]$$

$$= e^{-i\tau}\Big[r(e^{i\tau}V(t_{n+1},x_j)) - r(e^{i\tau}V(t_n,x_j))\Big] + e^{-i\tau}\Big[r(e^{i\tau}V(t_n,x_j)) - r(e^{i\tau}V_j^n)\Big]$$

$$= \int_{t_n}^{t_{n+1}} r'(e^{i\tau}V(t,x_j))\partial_t V(t,x_j)dt + \mathcal{E}_j^n \int_0^1 r'(e^{i\tau}V_j^n + te^{i\tau}\mathcal{E}_j^n)dt$$

$$=: (R_1)_j^n + \mathcal{E}_j^n (R_2)_j^n.$$

Hence, from (2.45), one can express the error $\mathcal{E}_j^{n+1}$ with respect to $\mathcal{E}_j^n$ and $\mathcal{E}_{j-1}^n$

$$\mathcal{E}_j^{n+1} = Q_j^{-1}\left[\left(1 - \frac{c\Delta t}{\Delta x} - (R_2)_j^n \Delta t\right)\mathcal{E}_j^n + \frac{c\Delta t}{\Delta x}\mathcal{E}_{j-1}^n + \Delta t g_j^n\right], \quad (2.46)$$

where Q_j is given by (2.42) and $g_j^n = -(R_1)_j^n + (R_x)_j^n + (R_t)_j^n - c\int_{t_n}^{t_{n+1}} \partial_{xt}^2 V(t,x_j)dt$. First, using Theorem 2.1 and the assumption on r, one has

$$\begin{aligned}\|g_j^n\|_{L_\tau^\infty} &\leq \|(R_1)_j^n\|_{L_\tau^\infty} + \|(R_x)_j^n\|_{L_\tau^\infty} + \|(R_t)_j^n\|_{L_\tau^\infty} + C\Delta t\\ &\leq C\Delta t + C\Delta x + C\Delta t + C\Delta t, \end{aligned} \quad (2.47)$$

where C is some positive constant which does not depend on ε. Second, we now consider the L_τ^∞ norm of (2.46) and use (2.43) to get (under the CFL condition $c\Delta t < \Delta x$)

$$\begin{aligned}\|\mathcal{E}_j^{n+1}\|_{L_\tau^\infty} &\leq \left\|\left(1 - \frac{c\Delta t}{\Delta x} + (R_2)_j^n \Delta t\right)\mathcal{E}_j^n + \frac{c\Delta t}{\Delta x}\mathcal{E}_{j-1}^n + \Delta t g_j^n\right\|_{L_\tau^\infty}\\ &\leq \max_j \|\mathcal{E}_j^n\|_{L_\tau^\infty} + \Delta t\|(R_2)_j^n\|_{L_\tau^\infty}\|\mathcal{E}_j^n\|_{L_\tau^\infty} + C\Delta t(\Delta t + \Delta x)\\ &\leq \|\mathcal{E}^n\|_{L_\tau^\infty}(1 + C\Delta t) + C\Delta t(\Delta t + \Delta x),\end{aligned}$$

where we denote by $\mathcal{E}^n = \max_{j=0,\ldots,N_x} |\mathcal{E}_j^n|$. A discrete Gronwall lemma enables one to get the required uniform estimate

$$\|\mathcal{E}^n\|_{L_\tau^\infty} \leq C(\Delta t + \Delta x)\exp(CT).$$

$\square$

Remark 2.8. *Higher order methods can be constructed by expanding to higher power in ε in the Chapman-Enskog expansion presented in subsection 2.3 and using higher order approximation scheme in time and space. We will not elaborate on this further in this paper.*

2.5 The cases where the oscillations come from both initial data and sources

In this part, we discuss the case where we may have high-oscillations in both the non linear PDE model and in the initial data. This corresponds to cases

where we have a model of type (2.1) with $a \neq 0$ and $u(0,x) = f_{in}(x, \beta(x)/\varepsilon)$, the function $f_{in} = f_{in}(x, \tau)$ being periodic in τ. The previous strategy cannot be applied in this general case and the uniform boundness of time and space derivatives of V at arbitrary order is no more garanteed. However, we can ensure that the first time and space derivatives are uniformly bounded.

The case of one-mode initial data In this case, the initial condition in (2.1) takes the form $u(0,x) = f_{in}(x, \beta(x)/\varepsilon) = \alpha(x)e^{i\beta(x)/\varepsilon}$. If we follow the analysis above and try to transform the equation on u into equations on the profile V and the oscillation phase S, then the only possibility to ensure some minimal smoothness on the augmented problem (2.6) and (2.4) is the following choice of the initial data

$$V(0,x,\tau) = \alpha(x), \qquad S(0,x) = \beta(x). \tag{2.48}$$

In particular, the initial data for V belong to the kernel of ∂_τ, and, according to the previous analysis, this only ensures that the first time and space derivatives are bounded. However, it is not possible to construct "well-prepared initial data" $V(0,x,\tau)$ so that high order time-space derivatives are also uniformly bounded.

The case of multi-modes initial data In this case, we expand the initial data as $f_{in}(x, \beta(x)/\varepsilon) = \sum_k f_k(x)e^{ik\beta(x)/\varepsilon}$ and one may decompose the solution as $u(t,x) = \sum_k u_k(t,x)$, where each component u_k satisfies

$$\partial_t u_k + c(x)\partial_x u_k + r(u)\delta_{1k} = \frac{ia(x)}{\varepsilon}u_k, \qquad u_k(0,x) = f_k(x)e^{ik\beta(x)/\varepsilon},$$

and δ_{ij} is the usual Kronecker symbol.

One can then apply the previous strategy, by considering the augmented functions $U_k(t,x,\tau)$ satisfying $U_k(t,x,kS(t,x)/\varepsilon) = u_k(t,x)$. This gives

$$\partial_t U_k + c(x)\partial_x U_k + \frac{1}{\varepsilon}[\partial_t S + c(x)\partial_x S]\partial_\tau U_k + r(U)\delta_{1k} = \frac{ia(x)}{\varepsilon}U_k, \ \ U_k(0,x,\tau) = f_k(x)e^{i\tau},$$

from which we deduce the equation for the phase S

$$\partial_t S + c(x)\partial_x S = a(x), \ \ S(0,x) = \beta(x),$$

and for U_k

$$\partial_t U_k + c(x)\partial_x U_k + r(U)\delta_{1k} = -\frac{a(x)}{\varepsilon}[\partial_\tau U_k - iU_k], \ \ U_k(0,x,\tau) = f_k(x)e^{i\tau}.$$

2.6 The full numerical algorithms

In this section, details of the algorithm for solving V and S are given. Periodic boundary conditions are considered in the x and τ directions. The uniform

grids in time and space are defined as previously. In addition, we also use a uniform mesh for the τ direction: $\tau_\ell = \ell\Delta\tau$, for $\ell = 0, \ldots, N_\tau, \Delta\tau = 2\pi/N_\tau$. In the following description, the variable τ is kept continuous for simplicity. In our numerical experiments, the pseudo spectral method is used for this variable. We denote by $V_j^n(\tau) \approx V(t^n, x_j, \tau)$ and $S_j^n \approx S(t^n, x_j)$ the discrete unknowns.

We start with V_j^0 given by (2.14) and $S_j^0 = 0$. Then, for all $n \geq 0$, the scheme reads (assuming $c > 0$)

$$\frac{V_j^{n+1} - V_j^n}{\Delta t} + c\frac{V_j^n - V_{j-1}^n}{\Delta x} + e^{-i\tau}r(e^{i\tau}V_j^n) = -\frac{a(x_j)}{\varepsilon}\partial_\tau V_j^{n+1},$$

$$\frac{S_j^{n+1} - S_j^n}{\Delta t} + c\frac{S_j^n - S_{j-1}^n}{\Delta x} = a(x_j).$$

At the final time $t_f = N\Delta t$ of the simulation, we come back to the original solution u through

$$u(t_f, x_j) = V_j^N\left(\tau = \frac{S_j^N}{\varepsilon}\right). \tag{2.49}$$

Since S_j^N/ε does not coincide with a grid point τ_ℓ, a trigonometric interpolation is performed. Note that higher order numerical schemes can be used and are necessary since one needs to obtain S_j^N/ε which may lead to large error in (2.49) if S is not computed accurately. *In practice we will use the pseudo-spectral method in x to solve the equation for S.*

2.7 Numerical tests

We present some tests solving (2.1) with $r(u) = u^2/(u^2 + 2|u|^2)$, $c(x) = \cos^2(x)$, $a(x) = 3/2 + \cos(2x) > 0$ and the following non-oscillatory initial data

$$u(0, x) = 1 + \frac{1}{2}\cos(2x) + i\left[1 + \frac{1}{2}\sin(2x)\right], \quad x \in I = [-\pi/2, \pi/2].$$

We compare the solution obtained by a direct method with resolved numerical parameters (smaller than ε) and the solution obtained by the new approach presented previously. The numerical parameters are as follows: $\Delta t = \Delta x/2 = |I|/N$ ($|I|$ being the length of the interval I) with $N = N_{ts}$ for the new approach and $N = N_d$ for the direct approach. We choose $N_\tau = 64$.

In Figures 1, 2, 3 and 4, we plot the ℓ^∞ error in space (as a function of a range of N_{ts}) between a reference solution obtained by a direct method with resolved numerical parameters and the solution obtained by the new method. The error is computed for different values of ε, at the final time $t_f = 0.1$, in different configurations.

In Figure 1, the initial data is well-prepared (given by (2.14)) and an exact solution for S is considered. We observe on the left part of Figure 1 that for different values of ε ($\varepsilon = 1, \ldots, 10^{-3}$), the new method is uniformly first order accurate both in space and time. On the right part of Figure 1, the error is plotted as a function of ε, for different values of N_{ts} ($N_{ts} = 20, 40, 100, 200, 1000$);

each curve, corresponding to a given N_{ts}, is almost constant, indicating that the error is independent from ε.

In Figure 2, the initial data is well-prepared (given by (2.14)) but we now consider a numerical calculation of the phase S. We used a first order upwind scheme together with a first order time integrator to compute S. Hence, a numerical error $\mathcal{O}(\Delta x + \Delta t)$ is generated on S, which is divided by ε to construct the approximation of $u(t_f, x_j)$. This explains the behavior of the curve associated to $\varepsilon = 10^{-3}$ for instance, in the left part of Figure 2. This is also emphasized on the right part of Figure 2: even if the curves do not cross each other, the error increases as ε decreases. To improve this, the numerical scheme for S is changed to a pseudo-spectral method in space with a fourth-order Runge-Kutta time integrator. The corresponding results are displayed in Figure 3. We observe that, since the error on S is now very small, the uniform accuracy is recovered.

In Figure 4, an exact calculation of the phase S is considered but now the initial data $V_j^0 = u(0, x_j)$ is not a corrected one . As expected (see [8, 7]), the uniform accuracy is lost since the error depends on ε, but we can observe that the numerical error is still small even for small ε.

In Figure 5, the same diagnostics as before are displayed, but we explore the possibility for a to *vanish* at isolated points by considering $a(x) = 1 + \cos(2x)$. With this choice of a, Theorem 2.4 does not apply directly. We consider the case with a corrected initial data and an exact calculation for S. The same results as before are obtained in the case of vanishing a: the new method is first order uniformly accurate in ε.

Then, we consider the asymptotic model given by (2.15) for which a standard numerical approximation (first order upwind scheme in space and first order explicit time integrator) is used to get $\bar{u}(t_f, x)$. Then, the quantity $e^{-iS(t_f, x)/\varepsilon}\bar{u}(t_f, x)$ is computed where the phase S is solved exactly. In Figure 6, the error (ℓ^∞ in space) between $e^{-iS(t_f, x)/\varepsilon}\bar{u}(t_f, x)$ and the solution of the new method is displayed as a function of ε (logarithmic scale). The error between the two models is $\mathcal{O}(\varepsilon)$. This numerically justifies Remark 2.3.

Finally, in Figures 7 and 8, we illustrate the space-time oscillations arising in the solution, with $a(x) = 3/2 + \cos(2x) > 0$. In Figure 7, the space dependence of the real part of the solution $u(t_f = 1, x)$ is displayed for $\varepsilon = 5 \cdot 10^{-3}$. A reference solution (obtained by a direct method with resolved numerical parameters $N_d = 4000$ and $\Delta t = 5 \cdot 10^{-4}$) and the solution obtained by the new approach (with $N_{ts} = 100$ and $\Delta t = \pi/200 \approx 0.0157$, $N_\tau = 16$, well-prepared initial data and an exact S) are plotted in the left part of Figure 7 (the right being a zoom of the left part). We can observe that the new method is able to capture very well high oscillations in space.

In Figure 8, we focus on time oscillations by considering the following time dependent quantity (root mean square type)

$$\mathcal{R}(t) = \left| \int_I u(t, x) x \, dx \right|.$$

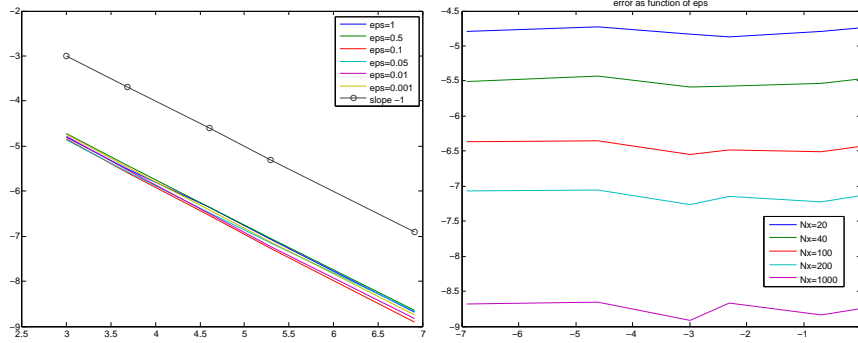The numerical quadrature for the reference solution is performed on the mesh

Figure 1: Plot of the ℓ^∞ error for the new method *with* corrected initial condition and exact computation for S. Left: error (log-log scale) as a function of N_{ts} ($N_{ts} = 20, 40, 100, 200, 1000$) for different values of ε ($\varepsilon = 1, \ldots, 10^{-3}$). Right: error (log-log scale) as a function of ε for different N_{ts}.
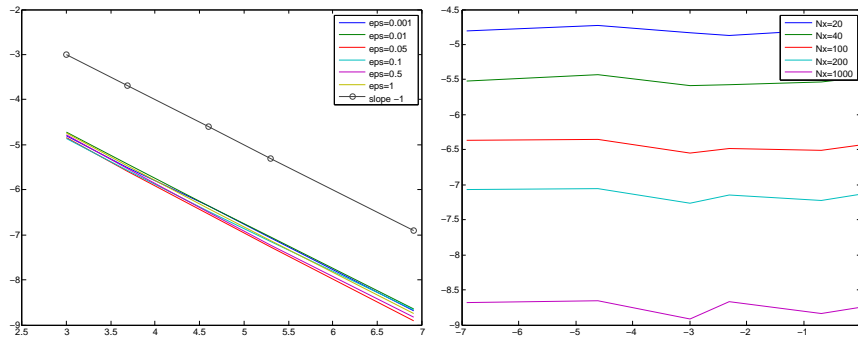
used for the new method. Using the same parameters as before, one can observe that the solution of the new method fits very well with the reference solution even when the oscillations are not resolved by the time step $\Delta t \approx 0.0157$. The right part of Figure 8 is a zoom of the left part.
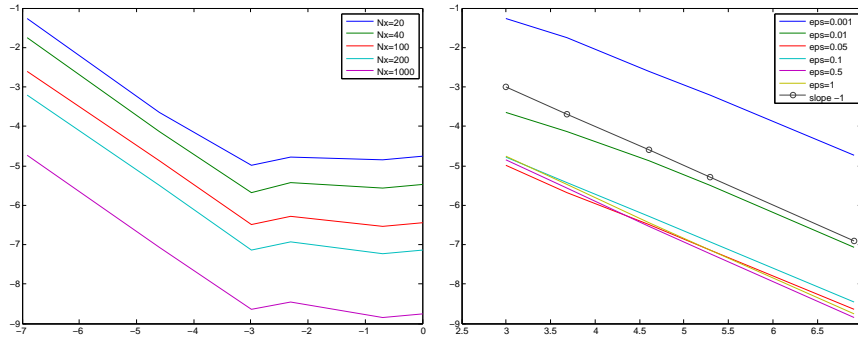
Figure 2: Plot of the ℓ^∞ error for the new method *with* corrected initial condition and numerical approximation for S. Left: error (log-log scale) as a function of N_{ts} ($N_{ts} = 20, 40, 100, 200, 1000$) for different values of ε ($\varepsilon = 1, \ldots, 10^{-3}$). Right: error (log-log scale) as a function of ε for different N_{ts}.

Figure 3: Plot of the ℓ^∞ error for the new method *with* corrected initial condition and an improved numerical approximation for S (pseudo-spectral in space and 4th order Runge-Kutta). Left: error (log-log scale) as a function of N_{ts} ($N_{ts} = 20, 40, 100, 200, 1000$) for different values of ε ($\varepsilon = 1, \ldots, 10^{-3}$). Right: error (log-log scale) as a function of ε for different N_{ts}.
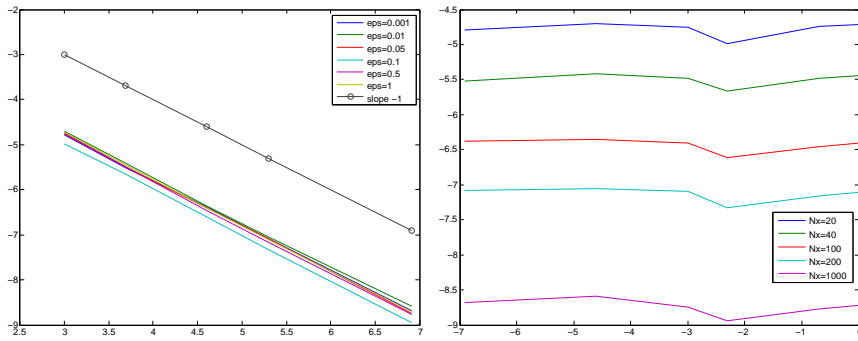
24
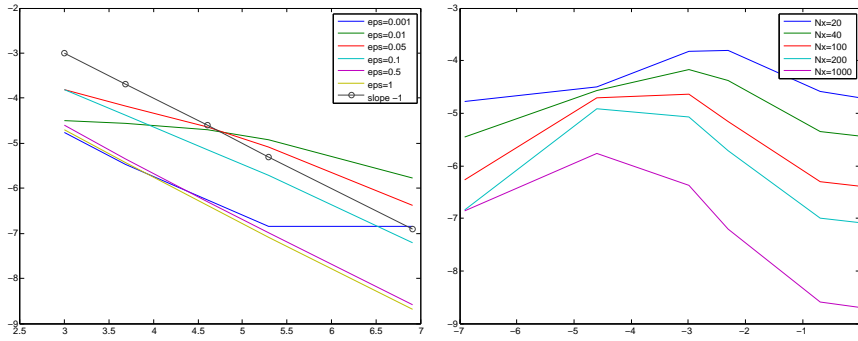
Figure 4: Plot of the ℓ^∞ error for the new method *without* corrected initial condition and exact computation for S. Left: error (log-log scale) as a function of N_{ts} ($N_{ts} = 20, 40, 100, 200, 1000$) for different values of ε ($\varepsilon = 1, \ldots, 10^{-3}$). Right: error (log-log scale) as a function of ε for different N_{ts}.

Figure 5: Plot of the ℓ^∞ error for the new method *with* corrected initial condition and exact computation for S, in the case where a vanishes ($a(x) = 1 + \cos(2x)$) at isolated points. Left: error (log-log scale) as a function of N_{ts} ($N_{ts} = 20, 40, 100, 200, 1000$) for different values of ε ($\varepsilon = 1, \ldots, 10^{-3}$). Right: error (log-log scale) as a function of ε for different N_{ts}.
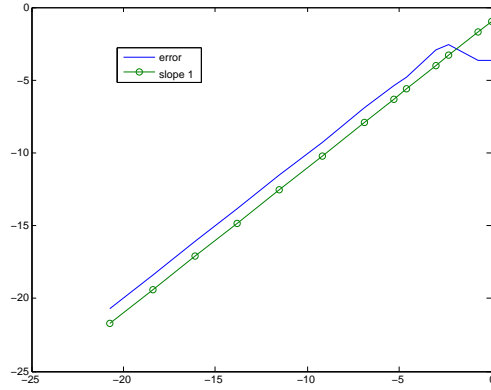
25

Figure 6: Plot of the ℓ^∞ error (log-log scale) between the solution of the asymptotic model (2.15) and the one obtained by the new method, as function of ε.
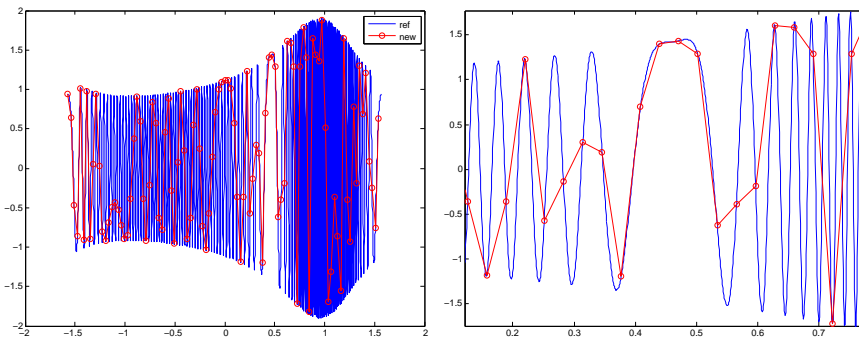

Figure 7: Comparison between a reference solution and the solution of the new method (*with* initial correction and exact computation for S), for $\varepsilon = 5 \cdot 10^{-3}$, $t_f = 1$. Left: space dependence of the real part of the unknown. The right part is a zoom of the left part.
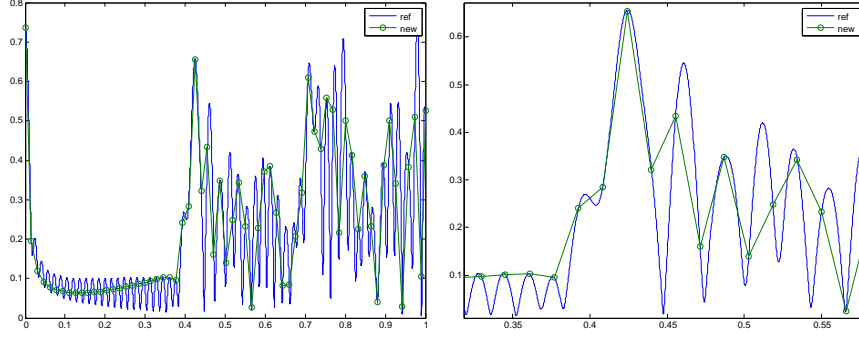
Figure 8: Time history of $\mathcal{R}$. Comparison between a reference solution and the solution of the new method (*with* initial correction and exact computation for S), for $\varepsilon = 5 \cdot 10^{-3}$, $t_f = 1$. The right part is a zoom of the left part.

3 Extension to a class of PDE systems

In this section, we focus on systems of equations and consider the case where $u(t, x) \in \mathbb{C}^2$ satisfies a hyperbolic system of the following form (with $t \geq 0, x \in \mathbb{R}$)

$$\partial_t u + A(x)\partial_x u + R(u) = \frac{iE(t,x)}{\varepsilon}Du + Cu, \quad u(t=0,x) = u_0(x), \qquad (3.1)$$

where $R(u) = (R_1(u), R_2(u)) \in \mathbb{C}^2$ is a reaction term, E is a real scalar function, C is a 2×2 constant matrix and

$$A(x) = \begin{pmatrix} a_1(x) & 0 \\ 0 & a_2(x) \end{pmatrix}, \quad D = \begin{pmatrix} 0 & 0 \\ 0 & -1 \end{pmatrix}, \quad C = \begin{pmatrix} C_{11} & C_{12} \\ C_{21} & C_{22} \end{pmatrix}.$$

This model is a simplified version of a more physical model to be studied in section 3.5.

3.1 GO versus NGO

We first show that the GO approach does not work for systems like (3.1), even in the linear case $R = 0$ and a non-oscillatory initial data $u(0,x) = u_0(x)$. This is due to the non-commutativeness of the matrices C and D in general. Indeed, let $u_k(t,x) = \alpha_k(t,x)e^{iS_k(t,x)/\varepsilon}, k = 1, 2$. Inserting this ansatz in (3.1), one gets

$$\partial_t \alpha_1 + a_1 \partial_x \alpha_1 + \frac{i}{\varepsilon}[\partial_t S_1 + a_1 \partial_x S_1]\alpha_1 = C_{11}\alpha_1 + C_{12}\alpha_2 e^{i(S_2-S_1)/\varepsilon},$$

$$\partial_t \alpha_2 + a_2 \partial_x \alpha_2 + \frac{i}{\varepsilon}[\partial_t S_2 + a_2 \partial_x S_2]\alpha_2 = -\frac{iE}{\varepsilon}\alpha_2 + C_{21}\alpha_1 e^{i(S_1-S_2)/\varepsilon} + C_{21}\alpha_2.$$

Set

$$\partial_t S_1 + a_1 \partial_x S_1 = 0, \qquad S_1(0,x) = 0,$$
$$\partial_t S_2 + a_2 \partial_x S_2 = -E, \qquad S_2(0,x) = 0,$$

27

thus $S_1(t,x) \equiv 0$, while $\alpha = (\alpha_1, \alpha_2)^T$ is governed by

$$\partial_t \alpha + A(x)\partial_x \alpha = B\alpha,$$

with

$$B = \begin{pmatrix} C_{11} & C_{12}e^{i(S_2 - S_1)/\varepsilon} \\ C_{21}e^{i(S_1 - S_2)/\varepsilon} & C_{22} \end{pmatrix}.$$

Clearly a solution α of this equation will be highly-oscillatory for ε small, whereas the GO ansatz assumes that α and S are smooth. Therefore the GO approach does not serve our goal. This motivates the NGO approach.

To do so, we consider the augmented function $U(t, x, \tau)$ such that

$$U(t, x, S(t,x)/\varepsilon) = u(t,x).$$

Then, $U = (U_1, U_2)$ satisfies

$$\partial_t U_1 + a_1 \partial_x U_1 + \frac{1}{\varepsilon}[\partial_t S + a_1 \partial_x S]\partial_\tau U_1 + R_1(U_1, U_2) = C_{11}U_1 + C_{12}U_2,$$

$$\partial_t U_2 + a_2 \partial_x U_2 + \frac{1}{\varepsilon}[\partial_t S + a_2 \partial_x S]\partial_\tau U_2 + R_2(U_1, U_2) = -\frac{iE}{\varepsilon}U_2 + C_{21}U_1 + C_{22}U_2.$$

The equation for the phase S writes

$$\partial_t S + a_2 \partial_x S = -E, \quad S(0, x) = 0,$$

and the equations for (U_1, U_2) become

$$\partial_t U_1 + a_1 \partial_x U_1 + \frac{1}{\varepsilon}[(a_1 - a_2)\partial_x S - E]\partial_\tau U_1 + R_1(U_1, U_2) = C_{11}U_1 + C_{12}U_2,$$

$$\partial_t U_2 + a_2 \partial_x U_2 + R_2(U_1, U_2) = -\frac{E}{\varepsilon}[\partial_\tau U_2 + iU_2] + C_{21}U_1 + C_{22}U_2.$$

Setting $V_2 = e^{i\tau}U_2$, we finally obtain

$$\begin{cases} \partial_t U_1 + a_1 \partial_x U_1 + R_1(U_1, e^{-i\tau}V_2) - C_{11}U_1 - C_{12}e^{-i\tau}V_2 = \frac{1}{\varepsilon}[E - (a_1 - a_2)\partial_x S]\partial_\tau U_1, \\[2em] \partial_t V_2 + a_2 \partial_x V_2 + e^{i\tau}R_2(U_1, e^{-i\tau}V_2) - C_{21}e^{i\tau}U_1 - C_{22}V_2 = -\frac{E}{\varepsilon}\partial_\tau V_2. \end{cases}$$

$$(3.2)$$

3.2 A suitable initial data for system (3.2)

Equation (3.2) needs initial data $U_1(0, x, \tau)$ and $V_2(0, x, \tau)$. This initial data $U(0, x, \tau)$ will be chosen such that the two following conditions are satisfied:

- $U(0, x, 0) = u_0(x) = (f_1^{in}(x), f_2^{in}(x))$.

- The solution to (3.2) is smooth with respect to ε: the successive derivatives in *time and space* (up to some order $p \geq 1$) are bounded uniformly in ε.

The approach is similar to the scalar case, and similar notations will be used in the following analysis.

We decompose the solutions U_1 and V_2 as $U_1 = U_1^0 + U_1^1$ and $V_2 = V_2^0 + V_2^1$, where $U_1^0 = \Pi U_1$ and $V_2^0 = \Pi V_2$. Injecting the decomposition into (3.2) and applying $(I - \Pi)$ to (3.2), one gets

$$
\begin{cases}
\partial_t U_1^1 + a_1 \partial_x U_1^1 + (\mathcal{I} - \Pi)[R_1(U_1, e^{-i\tau} V_2)] - C_{11} U_1^1 - C_{12}(\mathcal{I} - \Pi)[e^{-i\tau} V_2] \\
\qquad\qquad\qquad = -\dfrac{1}{\varepsilon}\left[E + (a_1 - a_2)\partial_x S\right] \partial_\tau U_1^1, \\[2mm]
\partial_t V_2^1 + a_2 \partial_x V_2^1 + (\mathcal{I} - \Pi)[e^{i\tau} R_1(U_1, e^{-i\tau} V_2)] - C_{21}(\mathcal{I} - \Pi)[e^{i\tau} U_1] - C_{22} V_2^1 \\[2mm]
\qquad\qquad\qquad = -\dfrac{E}{\varepsilon}\partial_\tau V_2^1.
\end{cases}
$$
(3.3)

Assuming for simplicity that $R_1 = R_2 = 0$, this implies that

$$
U_1^1 = \frac{\varepsilon C_{12}}{E + (a_1 - a_2)\partial_x S}\mathcal{L}^{-1}\left(e^{-i\tau}\right) V_2^0 + O(\varepsilon^2),
$$

$$
V_2^1 = -\frac{\varepsilon C_{21}}{E}\mathcal{L}^{-1}\left(e^{i\tau}\right) U_1^0 + O(\varepsilon^2),
$$

which explicitly gives (using $\mathcal{L}^{-1}(e^{\pm i\tau}) = \mp i e^{\pm i\tau}$)

$$
U_1^1 = \frac{i\varepsilon C_{12} e^{-i\tau}}{E + (a_1 - a_2)\partial_x S} V_2^0 + O(\varepsilon^2), \quad V_2^1 = -\frac{i\varepsilon C_{21} e^{i\tau}}{E} U_1^0 + O(\varepsilon^2).
$$

This yields

$$
U_1(t, x, \tau) = U_1^0(t, x) + \frac{i\varepsilon C_{12} e^{-i\tau}}{E(t, x) + (a_1(x) - a_2(x))\partial_x S(t, x)} V_2^0(t, x) + O(\varepsilon^2),
$$

$$
U_2(t, x, \tau) = V_2^0(t, x) e^{-i\tau} - \frac{i\varepsilon C_{21}}{E(t, x)} U_1^0(t, x) + O(\varepsilon^2).
$$

To find the suitable initial condition for U_1 and V_2, one uses $U_k(t = 0, x, 0) = f_k^{in}(x), k = 1, 2$, so that one needs to solve the following system in $(U_1^0, V_2^0)(0, x)$

$$
U_1^0(0, x) + \frac{i\varepsilon C_{12}}{E(0, x)} V_2^0(0, x) = f_1^{in}(x), \quad V_2^0(0, x) - \frac{i\varepsilon C_{21}}{E(0, x)} U_1^0(0, x) = f_2^{in}(x).
$$

The solutions are

$$
U_1^0 = \frac{1}{E^2 - \varepsilon^2 C_{21} C_{12}}\left(E^2 f_1^{in} - i C_{12}\varepsilon E f_2^{in}\right)
$$

$$
V_2^0 = \frac{1}{E^2 - \varepsilon^2 C_{21} C_{12}}\left(i\varepsilon C_{21} E f_1^{in} + E^2 f_2^{in}\right).
$$

Thus, the initial conditions with first order correction writes

$$
\begin{cases}
U_1(0, x, \tau) = f_1^{in} + \dfrac{i\varepsilon E C_{12}}{E^2 - \varepsilon^2 C_{12} C_{21}} \left(e^{-i\tau} - 1 \right) f_2^{in}, \\[4mm]
U_2(0, x, \tau) = \dfrac{i\varepsilon E C_{21}}{E^2 - \varepsilon^2 C_{12} C_{21}} \left(e^{-i\tau} - 1 \right) f_1^{in} + e^{-i\tau} f_2^{in}.
\end{cases}
\tag{3.4}
$$

3.3   A numerical scheme for the 2×2 system (3.2)

Denoting $U_1^n(x, \tau) \approx U_1(t^n, x, \tau)$ and $V_2^n(x, \tau) \approx V_2(t^n, x, \tau)$ the approximations of the solution to (3.2) which satisfy the following numerical (semi-discrete in time) scheme

$$
\begin{cases}
\dfrac{U_1^{n+1} - U_1^n}{\Delta t} + a_1 \partial_x U_1^n - C_{11} U_1^n - C_{12} e^{-i\tau} V_2^n \\[4mm]
\qquad\qquad\qquad\qquad\qquad = -\dfrac{1}{\varepsilon} \left[E^n + (a_1 - a_2) \partial_x S^n \right] \partial_\tau U_1^{n+1}, \\[4mm]
\dfrac{V_2^{n+1} - V_2^n}{\Delta t} + a_2 \partial_x V_2^n - C_{21} e^{i\tau} U_1^n - C_{22} V_2^n = -\dfrac{E^n}{\varepsilon} \partial_\tau V_2^{n+1},
\end{cases}
\tag{3.5}
$$

whereas for the phase S, we use

$$
\frac{S^{n+1} - S^n}{\Delta t} + a_2 \partial_x S^n = -E^n.
$$

At initial time $n = 0$, we use the corrected initial condition (3.4). For the space approximation, we use the psuedo-spectral scheme in the periodic variable τ and a first order upwind scheme for the transport terms in x (high order methods will be used for the approximation of S (as discussed in the scalar case), as well as semi-Lagrangian method). Then, from $(U_1^n(x, \tau), V_2^n(x, \tau), S^n(x))$, we can construct an approximation of $u(t^n, x) = (u_1(t^n, x), u_2(t^n, x))$ solution to (3.1) through the relation

$$
u_1(t^n, x) = U_1^n(x, \tau = S^n(x)/\varepsilon), \quad u_2(t^n, x) = e^{-iS^n(x)/\varepsilon} V_2^n(x, \tau = S^n(x)/\varepsilon),
$$

where the evaluation at $\tau = S^n(x)/\varepsilon$ is performed by trigonometric interpolation since the solution are periodic with respect to the τ variable.

3.4   Numerical results

This section is devoted to numerical illustration of the new approach for the case of 2x2 systems. We solve (3.1) with $a_1(x) = 1, a_2(x) = 4, R(u) = 0, E(t, x) = 3/2 + \cos(x)$, and

$$
C = \begin{pmatrix} 0 & 1 \\ -1 & 0 \end{pmatrix}.
$$

We consider the following initial condition

$$u(t=0,x) = \left(1 + \frac{1}{2}\cos(x) + i\sin(x), 1 + \frac{1}{2}\cos(x) + i\sin(x)\right), \quad x \in [0, 2\pi].$$

As in the scalar case, we compare the solution obtained by a direct method (time splitting with exact (in time) integration of each substep) and by the new approach. The direct method uses resolved parameters so its solution provides a reference which will be compared to the solution of the new method. For this latter method, the following numerical parameters are used: $\Delta x = 2\pi/N_{ts}, \Delta t = \Delta x/(2\max(a_1, a_2)), N_\tau = 64$, where N_{ts} is the number of (uniform) grid points in the spatial direction.

In the following figures, we are interested in the ℓ^∞ error in space (for different values of N_{ts}) at the final time $t_f = 0.1$, between the new method and the reference solution, for different values of ε.

In Figure 9, the solution obtained with the new method is computed with the corrected initial condition and with an exact solution for the phase S. We plot the ℓ^∞ error for different values of ε as a function of N_{ts} (left part) and the ℓ^∞ error as a function of ε for different N_{ts} (right part). As in the scalar case, the uniform accuracy is observed: the order of accuracy is independent of ε and the error is constant with respect to ε.

In Figure 10, we study the influence of the numerical approximation of S on the error. We used for the approximation of S a first order upwind scheme in space with a first order time integrator. We plot the same diagnostics as before. As in the scalar case, we observe a bad behavior when ε becomes small. Then, in Figure 11, we consider an improved numerical approximation of S by using a pseudo-spectral method in space with a 4th-order Runge-Kutta time integrator. We then observe that the uniform accuracy is recovered.

In Figure 12, an exact computation of S is used but the initial data is not corrected. Again, we plot the ℓ^∞ error. As expected the uniform accuracy is lost, in particular in the intermediate regime.

Finally, in the following figures, we illustrate the performances of the new method using the same data as before except the initial condition

$$u(t=0,x) = \left(1 + \frac{1}{2}\cos(x), 1 + \frac{1}{2}\cos(x)\right), \quad x \in [0, 2\pi].$$

We compare a reference solution (computed with a direct method using resolved numerical parameters $N_d = 4000, \Delta t = 10^{-4}$) and the solution of the new method at $t_f = 1$, for $\varepsilon = 0.01$. For the new method, we choose $N_\tau = 8$, a well-prepared initial condition, an exact phase S and different values of N_{ts} are considered. In Figure 13, we plot the real and imaginary part of the first component of the solution as a function of space for $N_{ts} = 20, 40, 100$ (and $\Delta t = 2\pi/(2N_{ts}\max(a_1, a_2))$). Even with a very coarse mesh, we observe that the new method is able to capture the high space oscillations of the solution. In Figure 14, the real part of the second component of the solution is displayed as a function of x, for $N_{ts} = 20, 40, 100$. On the right column (which is a zoom of the left one), we see that the new solution almost coincides with the reference

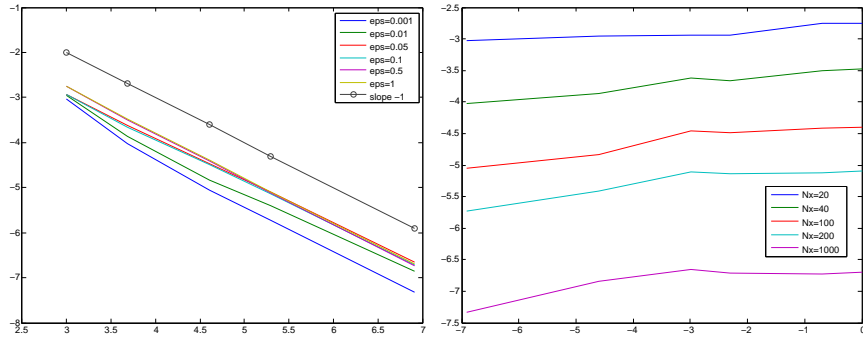Figure 9: Plot of the ℓ^∞ error for the new method *with* corrected initial condition and exact computation for S. Left: error (log-log scale) as a function of N_{ts} ($N_{ts} = 20, 40, 100, 200, 1000$) for different values of ε ($\varepsilon = 1, \ldots, 10^{-3}$). Right: error (log-log scale) as a function of ε for different N_{ts}.
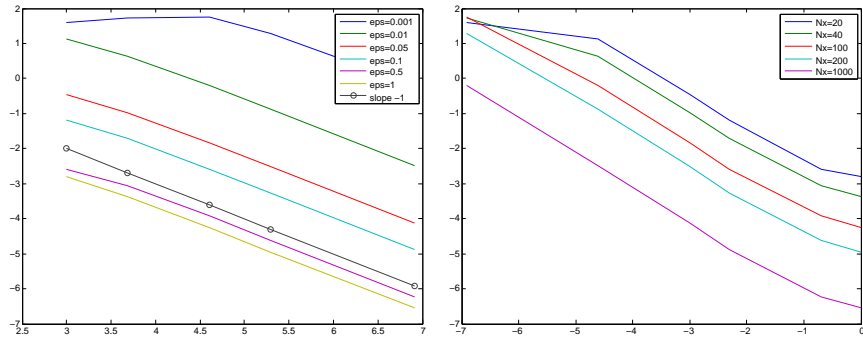

Figure 10: Plot of the ℓ^∞ error for the new method *with* corrected initial condition and numerical approximation for S. Left: error (log-log scale) as a function of N_{ts} ($N_{ts} = 20, 40, 100, 200, 1000$) for different values of ε ($\varepsilon = 1, \ldots, 10^{-3}$). Right: error (log-log scale) as a function of ε for different N_{ts}.
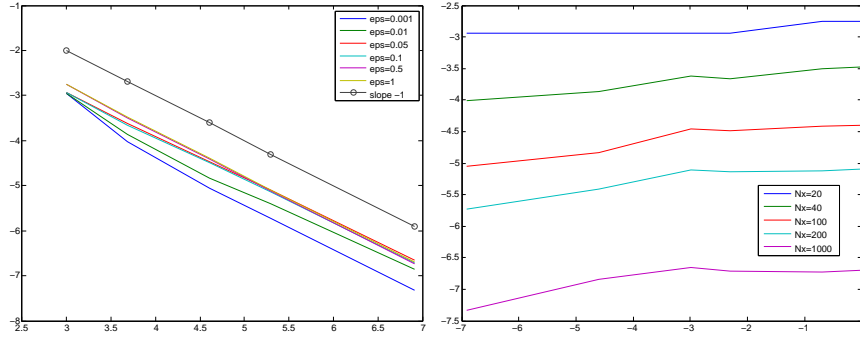
Figure 11: Plot of the ℓ^∞ error for the new method *with* corrected initial condition and an improved numerical approximation for S (pseudo-spectral in space and 4th order Runge-Kutta). Left: error (log-log scale) as a function of N_{ts} ($N_{ts} = 20, 40, 100, 200, 1000$) for different values of ε ($\varepsilon = 1, \ldots, 10^{-3}$). Right: error (log-log scale) as a function of ε for different N_{ts}.
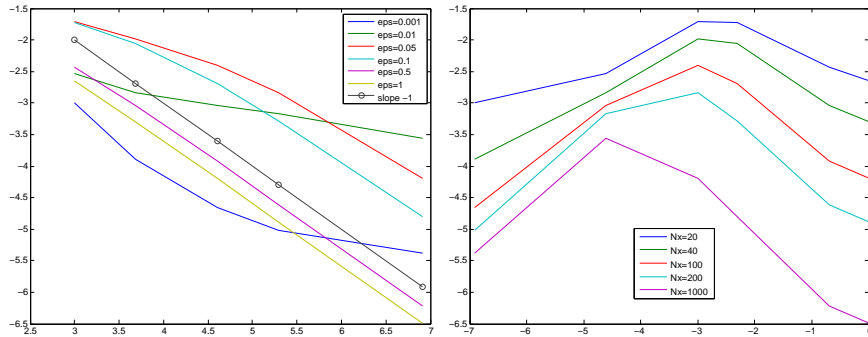

Figure 12: Plot of the ℓ^∞ error for the new method *without* corrected initial condition and an exact computation for S. Left: error (log-log scale) as a function of N_{ts} ($N_{ts} = 20, 40, 100, 200, 1000$) for different values of ε ($\varepsilon = 1, \ldots, 10^{-3}$). Right: error (log-log scale) as a function of ε for different N_{ts}.

one even if the spatial mesh $\Delta x \approx 0.31, 0.15, 0.06$ is large compared to the size of the smallest oscillations (of order $\varepsilon = 0.01$).

3.5   An application to a semiclassical surface hopping model

We now show that the general approach described above can be applied to efficiently solve the following semiclasscial surface hopping model, introduced in [6]:

$$
\begin{aligned}
\partial_t f^+ + p \cdot \nabla_x f^+ - \nabla_x(U + E) \cdot \nabla_p f^+ &= \overline{b}^i f^i + b^i \overline{f}^i, \\
\partial_t f^- + p \cdot \nabla_x f^- - \nabla_x(U - E) \cdot \nabla_p f^- &= -\overline{b}^i f^i - b^i \overline{f}^i, \\
\partial_t f^i + p \cdot \nabla_x f^i + \nabla_x U \cdot \nabla_p f^i &= -i\frac{2E}{\varepsilon} f^i + b^i(f^- - f^+) + (b^+ - b^-)f^i,
\end{aligned}
$$

$$(3.6)$$

where $(f^+(t, x, p), f^-(t, x, p), f^i(t, x, p)) \in \mathbb{R} \times \mathbb{R} \times \mathbb{C}$, $(t, x, p) \in \mathbb{R}_+ \times \mathbb{R}^d \times \mathbb{R}^d$, and $b^\pm \in \mathbb{C}, b^i \in \mathbb{C}, U \in \mathbb{R}, E \in \mathbb{R}$ are given functions depending only on the space variable x. We denote also by

$$
(f^+(0, x, p), f^-(0, x, p), f^i(0, x, p)) = (f^+_{in}(x, p), f^-_{in}(x, p), f^i_{in}(x, p))
$$

the initial conditions.

This model approximates semiclassically the nucleaonic Schrödinger system arising from the Born-Oppenheimer approximation with non-adiabatic corrections. The right hand side describes the interband transition between different potential energy surfaces ($2E$ is the *band gap* between two energy surfaces), and the coefficients are related to Berry connection. We refer to [6] for more details.

As explained above, the general idea is to introduce a phase $S(t, x, p)$ designed to follow the main oscillations in this model. We then consider the phase $S(t, x, p)$, solution to

$$
\partial_t S + p \cdot \nabla_x S + \nabla_x U \cdot \nabla_p S = 2E, \quad S(0, x, p) = 0, \tag{3.7}
$$

and introduce the augmented unknowns $(F^\pm, F^i)(t, x, p, \tau)$ satisfying

$$
f^\pm(t, x, p) = F^\pm(t, x, p, S(t, x, p)/\varepsilon), \quad f^i(t, x, p) = F^i(t, x, p, S(t, x, p)/\varepsilon).
$$

One then has:

$$
\begin{aligned}
\partial_t F^+ + p \cdot \nabla_x F^+ - \nabla_x(U + E) \cdot \nabla_p F^+ &= \\
\frac{-1}{\varepsilon} \left(2E - \nabla_x(2U + E) \cdot \nabla_p S\right) \partial_\tau F^+ + \overline{b}^i F^i + b^i \overline{F}^i, \\
\partial_t F^- + p \cdot \nabla_x F^- - \nabla_x(U - E) \cdot \nabla_p F^- &= \\
\frac{-1}{\varepsilon} \left(2E - \nabla_x(2U - E) \cdot \nabla_p S\right) \partial_\tau F^- - \overline{b}^i F^i - b^i \overline{F}^i, \\
\partial_t F^i + p \cdot \nabla_x F^i + \nabla_x U \cdot \nabla_p F^i &= \\
-\frac{2E}{\varepsilon} \left(\partial_\tau F^i + iF^i\right) + b^i(F^- - F^+) + (b^+ - b^-)F^i. \quad (3.8)
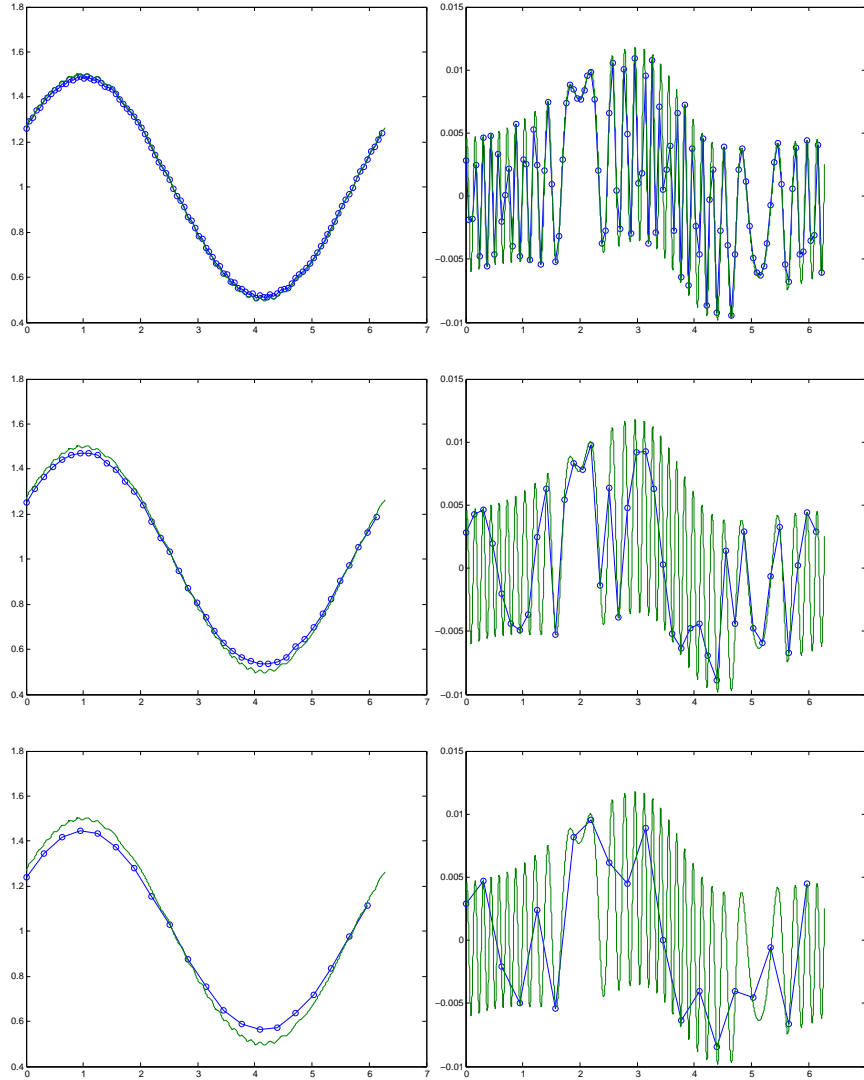\end{aligned}
$$

Figure 13: The first component of the solution (left column: real part, right column: imaginary part) as a function of x at time $t_f = 1$, $\varepsilon = 0.01$. Comparison between the reference solution (with $N_d = 4000, \Delta t = 10^{-4}$) and the new method with $N_{ts} = 100, 40, 20$ (from top to bottom).
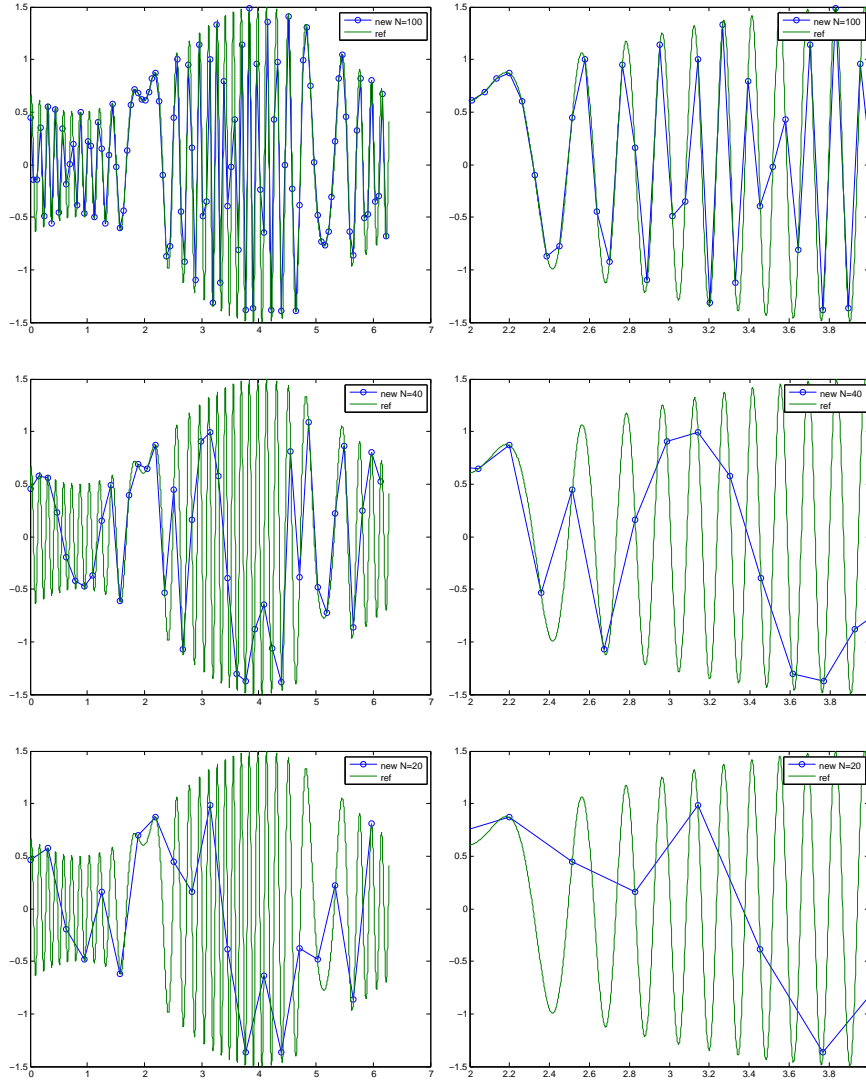
Figure 14: The real part of the second component of the solution as a function of x at time $t_f = 1$, $\varepsilon = 0.01$. Comparison between the reference solution (with $N_d = 4000, \Delta t = 10^{-4}$) and the new method with $N_{ts} = 100, 40, 20$ (from top to bottom).

Let $G^i = e^{i\tau} F^i$, then

$$\partial_t F^+ + p \cdot \nabla_x F^+ - \nabla_x (U + E) \cdot \nabla_p F^+ = -\frac{\mathcal{E}^+}{\varepsilon} \partial_\tau F^+ + \overline{b}^i e^{-i\tau} G^i + b^i e^{i\tau} \overline{G}^i,$$

$$\partial_t F^- + p \cdot \nabla_x F^- - \nabla_x (U - E) \cdot \nabla_p F^- = -\frac{\mathcal{E}^-}{\varepsilon} \partial_\tau F^- - \overline{b}^i e^{-i\tau} G^i - b^i e^{i\tau} \overline{G}^i,$$

$$\partial_t G^i + p \cdot \nabla_x G^i + \nabla_x U \cdot \nabla_p G^i = -\frac{2E}{\varepsilon} \partial_\tau G^i + b^i e^{i\tau} (F^- - F^+) + (b^+ - b^-) G^i,$$

(3.9)

where $\mathcal{E}^\pm = 2E - \nabla_x (2U \pm E) \cdot \nabla_p S$. This system needs initial data $F(0, x, p, \tau)$ and $G^i(0, x, p, \tau)$, which will be determined in a such way that the corresponding solution is smooth with respect to ε. We proceed as in Section 3.2 for the 2×2 model. Let

$$F_0^\pm = \Pi F^\pm, \quad F_1^\pm = (\mathcal{I} - \Pi) F^\pm, \quad G_0^i = \Pi G^i, \quad G_1^i = (I - \Pi) G^i.$$

We have
$$G^i = G_0^i - i\frac{\varepsilon}{2E} b^i e^{i\tau} (F_0^- - F_0^+) + O(\varepsilon^2),$$
$$F^+ = F_0^+ + i\frac{\varepsilon}{\mathcal{E}^+} \left(\overline{b}^i e^{-i\tau} G_0^i - b^i e^{i\tau} \overline{G}_0^i \right) + O(\varepsilon^2), \qquad (3.10)$$
$$F^- = F_0^- - i\frac{\varepsilon}{\mathcal{E}^-} \left(\overline{b}^i e^{-i\tau} G_0^i - b^i e^{i\tau} \overline{G}_0^i \right) + O(\varepsilon^2).$$

To fit with the initial data $(f_{in}^+, f_{in}^-, f_{in}^i)$, we set

$$G_0^i - i\frac{\varepsilon}{2E} b^i (F_0^- - F_0^+) = f_{in}^i,$$

$$F_0^+ + i\frac{\varepsilon}{\mathcal{E}^+} \left(\overline{b}^i G_0^i - b^i \overline{G}_0^i \right) = f_{in}^+,$$

$$F_0^- - i\frac{\varepsilon}{\mathcal{E}^-} \left(\overline{b}^i G_0^i - b^i \overline{G}_0^i \right) = f_{in}^-.$$

This gives

$$F_0^+ = f_{in}^+ - i\frac{\varepsilon}{\mathcal{E}^+} \left(\overline{b}^i f_{in}^i - b^i \overline{f}_{in}^i \right),$$

$$F_0^- = f_{in}^- + i\frac{\varepsilon}{\mathcal{E}^-} \left(\overline{b}^i f_{in}^i - b^i \overline{f}_{in}^i \right),$$

$$G_0^i = f_{in}^i - i\frac{\varepsilon}{2E} b^i (f_{in}^+ - f_{in}^-).$$

Reporting these expressions in (3.10) yields

$$F^+(0, x, p, \tau) = f_{in}^+ - i\frac{\varepsilon}{\mathcal{E}^+} \left(\overline{b}^i f_{in}^i \left(1 - e^{-i\tau}\right) - b^i \overline{f}_{in}^i \left(1 - e^{-i\tau}\right) \right),$$
$$F^-(0, x, p, \tau) = f_{in}^- + i\frac{\varepsilon}{\mathcal{E}^-} \left(\overline{b}^i f_{in}^i \left(1 - e^{-i\tau}\right) - b^i \overline{f}_{in}^i \left(1 - e^{-i\tau}\right) \right), \qquad (3.11)$$
$$G^i(0, x, p, \tau) = f_{in}^i + i\frac{\varepsilon}{2E} b^i \left(e^{i\tau} - 1\right) (f_{in}^+ - f_{in}^-).$$

3.6 Numerical results

We consider the following initial conditions for (3.6) with $x, v \in [-2\pi, 2\pi]$

$$f_+(t = 0, x, p) = f_-(t = 0, x, p) = (1 + 0.5\cos(x))\frac{e^{-p^2/2}}{\sqrt{2\pi}},$$

$$f_i(t = 0, x, p) = \left[(1 + 0.5\sin(x)) + i(1 + 0.5\cos(x))\right]\frac{e^{-p^2/2}}{\sqrt{2\pi}},$$

and the following expression for E, b_i and $b_\pm$

$$E(x) = 1 - \cos(x/2) + \varepsilon, \quad b_i(x, p) = -\frac{1}{2}\sin(p + 1), \quad b_\pm = 0.$$

Notice that with this choice of E, the narrowest band gap $2E = 2\varepsilon$ which describes the so-called "avoided-crossing" case (see [6]). We will compare a direct simulation of the model (3.6) (using time splitting and pseudo-spectral methods in space) with our new approach (3.9) (using time splitting, pseudo-spectral methods in space also and the well-prepared initial condition (3.11)). Moreover, periodic boundary conditions are considered in both x and p.

In the sequel, we detail the steps of the two methods (direct and new). First, we introduce the following notations: $\mathcal{A} = (-\nabla_x(U + E), -\nabla_x(U - E), \nabla_x U, \nabla_x U)$, and $\mathcal{E} = (-\mathcal{E}^+, -\mathcal{E}^-, -2E/\varepsilon, -2E/\varepsilon)$ whereas the matrix B_τ is given by

$$B_\tau = \begin{pmatrix} 0 & 0 & 2b^i\cos\tau & 2b^i\sin\tau \\ 0 & 0 & -2b^i\cos\tau & -2b^i\sin\tau \\ -b^i\cos\tau & b^i\cos\tau & 0 & 0 \\ -b^i\sin\tau & b^i\sin\tau & 0 & 0 \end{pmatrix},$$

and B by

$$B = \begin{pmatrix} 0 & 0 & 2b^i & 0 \\ 0 & 0 & -2b^i & 0 \\ -b^i & b^i & 0 & 2E/\varepsilon \\ 0 & 0 & -2E/\varepsilon & 0 \end{pmatrix}.$$

Then, the direct numerical scheme for (3.6) writes (with $f = (f^+, f^-, \mathrm{Re}(f^i), \mathrm{Im}(f^i)) \in \mathbb{R}^4$)

- solve $\partial_t f + p\partial_x f = 0$ with spectral method in space and exact integration in time,

- solve $\partial_t f + \mathcal{A}\partial_p f = 0$ with spectral method in space and exact integration in time,

- solve $\partial_t f = Bf$ (with B a 4x4 matrix given above) exactly in time.

The numerical scheme for (3.9) is (with $F = (F^+, F^-, \mathrm{Re}(G^i), \mathrm{Im}(G^i)) \in \mathbb{R}^4$)

- solve $\partial_t F + p\partial_x F = 0$ with spectral method in space and exact integration in time,

- solve $\partial_t F + \mathcal{A}\partial_p F = 0$ with spectral method in space and exact integration in time,

- solve $\partial_t F = B_\tau F$ (with B_τ a 4x4 matrix given above) exactly in time,

- solve $\partial_t F = \frac{1}{\varepsilon}\mathcal{E}\partial_\tau F$ with a pseudo-spectral method in τ and an implicit Euler scheme in time (exact time integration in the Fourier space can also be done).

The equation (3.7) on S is solved using a time splitting method (between transport and right hand side) and spectral methods are used in (x, p).

In Figure 15, we plot the space dependence of the solution $f(t_f = 2, x, p = 0)$ and of the densities $\rho(t_f = 2, x) = \int_{\mathbb{R}} f(t_f = 2, x, p)dp$, for $\varepsilon = 1$ for the direct and the new methods. The reference solution uses $\Delta t = 0.05$, $N_x = 256$, $N_p = 64$ whereas for the new method, we choose $\Delta t = 0.05$, $N_x = 32$, $N_p = 64$ and $N_\tau = 8$. First, we observe that the new method captures well the solution for both diagnostics. Second, the CPU time is about 15 s for the reference method whereas for the new method, it is about 1 min.

In Figures 16 and 17, we consider the same diagnostics as before, but with $\varepsilon = 1/32$. The reference solution uses now $\Delta t = 0.02$, $N_x = 512$, $N_p = 64$ whereas we still choose $\Delta t = 0.05$, $N_x = 32$, $N_p = 64$ and $N_\tau = 8$ for the new method. Then, the CPU time for the reference method is now 75 s and is still 1 min for the new method. Even for this value of ε, the solution is highly oscillatory (the f^i part in particular) and the new method behaves very well even its mesh is coarser than the spatial oscillations.

Finally, in Figures 18 and 19, we consider $\varepsilon = 1/256$ and $t_f = 0.2$. The numerical parameters for the reference method have been chosen to resolve the space-time oscillations ($\Delta t = 0.0005$, $N_x = 4096$, $N_p = 64$) so that the CPU time is 1420 s. The numerical parameters of the new method are still fixed (so as its CPU time). The same conclusions as before arise.

4 Conclusion

In this work, for a class of highly oscillatory hyperbolic systems of transport equations, we introduced a new numerical method which allows one to obtain accurate numerical solutions with mesh size and time step independent of the (possibly very small) wave length. The central ideas include a geometric optics based ansatz, which builds the oscillatory phase into an independent variable, and a suitably chosen initial data derived from the Chapman-Enskog expansion. For a scalar model we prove that a first order approximation the converges with a first order accuracy uniformly in the wave length, and the method is also extended for a system that arises in semiclassical modeling of surface hopping, which deals with quantum transition between different energy bands. Numerous numerical examples demonstrate that the method has the desired property of capturing the point-wise solutions of highly oscillatory waves with mesh sizes much larger than the wave length. .

In the future, we will extend the method to higher dimensions, conduct more theoretical investigation on the method for systems, and study other interesting non-adiabatic quantum dynamics problems.

References

[1] Anton Arnold, Naoufel Ben Abdallah, and Claudia Negulescu, *WKB-based schemes for the oscillatory 1D Schrödinger equation in the semiclassical limit*, SIAM J. Numer. Anal. **49** (2011), no. 4, 1436–1460. MR 2831055

[2] Weizhu Bao, Yongyong Cai, and Xiaofei Zhao, *A uniformly accurate multiscale time integrator pseudospectral method for the Klein-Gordon equation in the nonrelativistic limit regime*, SIAM J. Numer. Anal. **52** (2014), no. 5, 2488–2511. MR 3268616

[3] Weizhu Bao, Xuanchun Dong, and Xiaofei Zhao, *Uniformly accurate multiscale time integrators for highly oscillatory second order differential equations*, J. Math. Study **47** (2014), no. 2, 111–150. MR 3260336

[4] Weizhu Bao, Shi Jin, and Peter A. Markowich, *On time-splitting spectral approximations for the Schrödinger equation in the semiclassical regime*, J. Comput. Phys. **175** (2002), no. 2, 487–524. MR 1880116

[5] Carlo Cercignani, *The Boltzmann equation and its applications*, Applied Mathematical Sciences, vol. 67, Springer-Verlag, New York, 1988. MR 1313028

[6] Lihui Chai, Shi Jin, Qin Li, and Omar Morandi, *A multiband semiclassical model for surface hopping quantum dynamics*, Multiscale Model. Simul. **13** (2015), no. 1, 205–230. MR 3301305
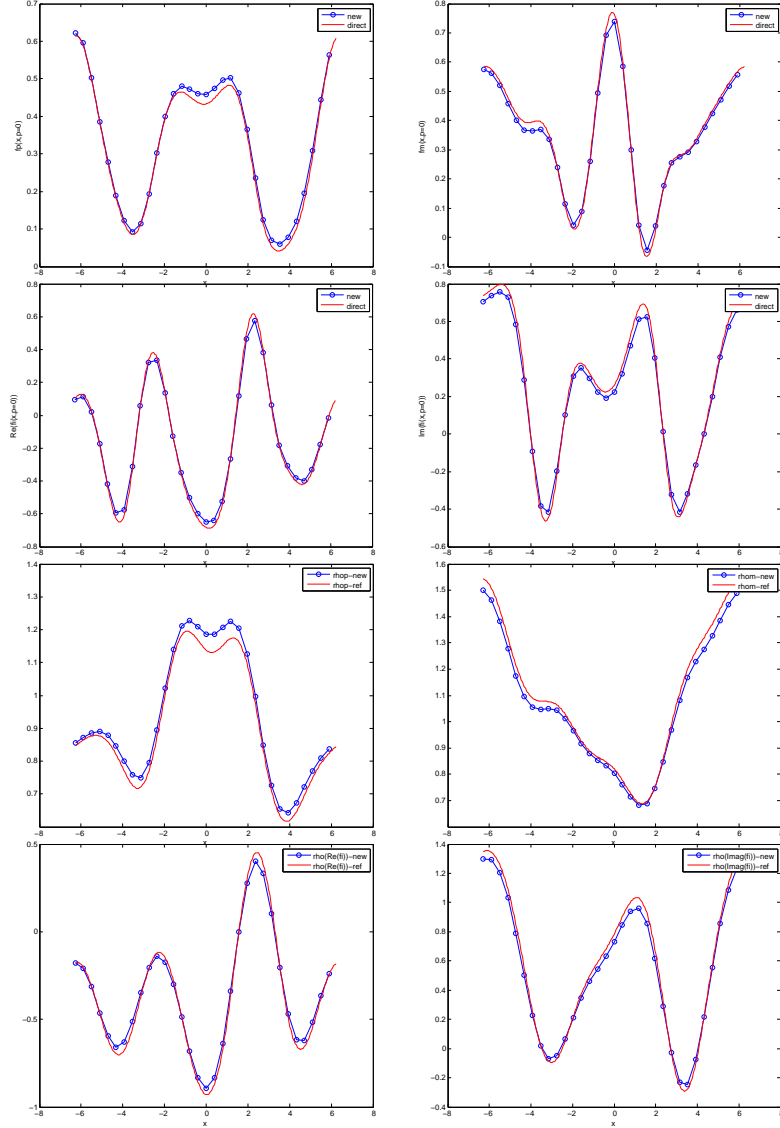
Figure 15: $\varepsilon = 1$. From top left to bottom right: space dependence of f^+, f^-, $\mathrm{Re}(f^i)$ and $\mathrm{Im}(f^i)$ at $p = 0$, and space dependence of the densities ρ^+, ρ^-, $\mathrm{Re}(\rho^i)$ and $\mathrm{Im}(\rho^i)$.
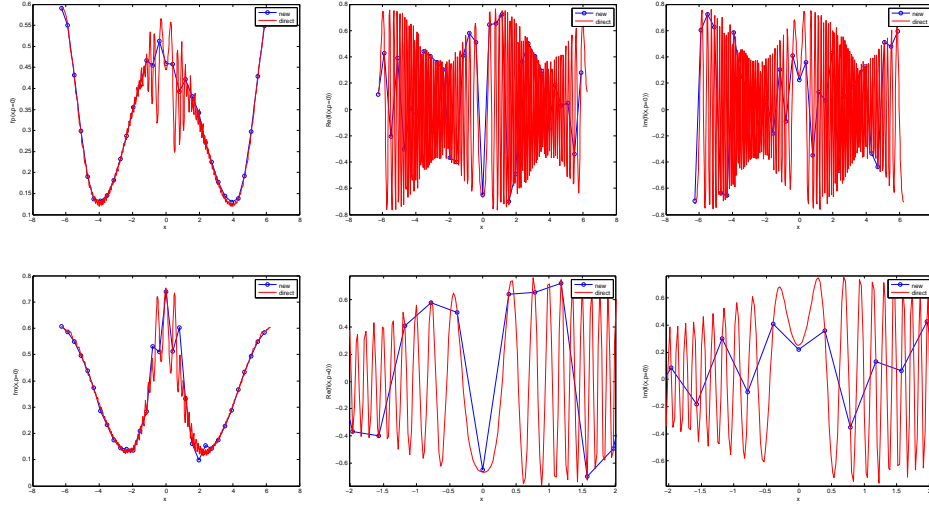
Figure 16: $\varepsilon = 1/32$. First line: space dependence of f^+, $\mathrm{Re}(f^i)$ and $\mathrm{Im}(f^i)$ at $p = 0$. Second line: space dependence of f^-, $\mathrm{Re}(f^i)$ (zoom) and $\mathrm{Im}(f^i)$ (zoom) at $p = 0$.
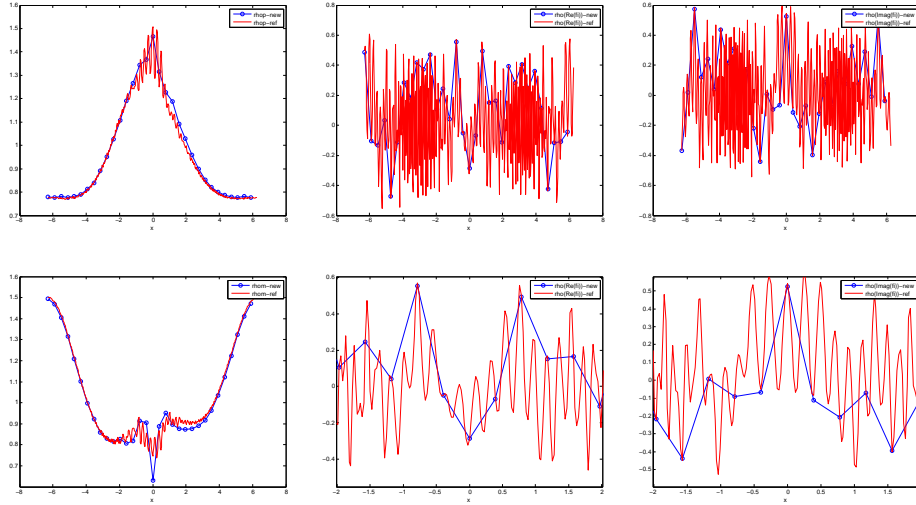

Figure 17: $\varepsilon = 1/32$. First line: space dependence of the densities ρ^+, $\mathrm{Re}(\rho^i)$ and $\mathrm{Im}(\rho^i)$. Second line: space dependence of ρ^-, $\mathrm{Re}(\rho^i)$ (zoom) and $\mathrm{Im}(\rho^i)$ (zoom).
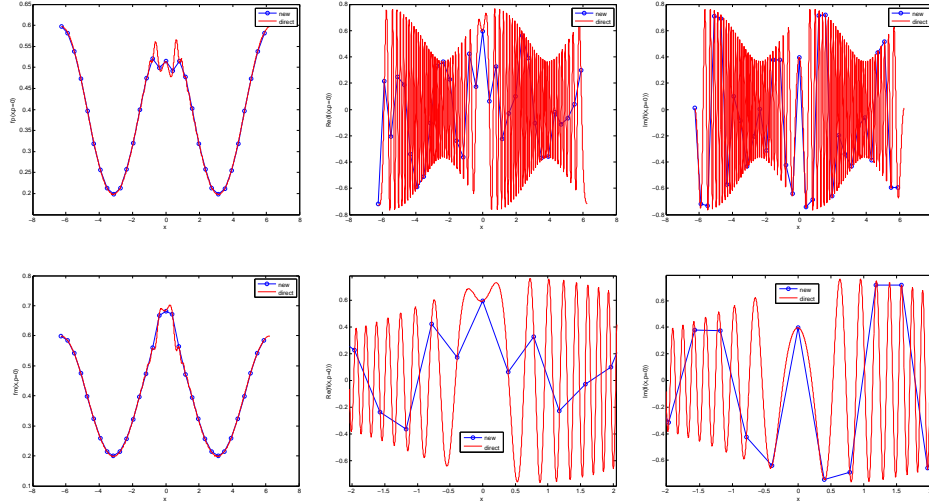
Figure 18: $\varepsilon = 1/256$. First line: space dependence of f^+, $\mathrm{Re}(f^i)$ and $\mathrm{Im}(f^i)$ at $p = 0$. Second line: space dependence of f^-, $\mathrm{Re}(f^i)$ (zoom) and $\mathrm{Im}(f^i)$ (zoom) at $p = 0$.
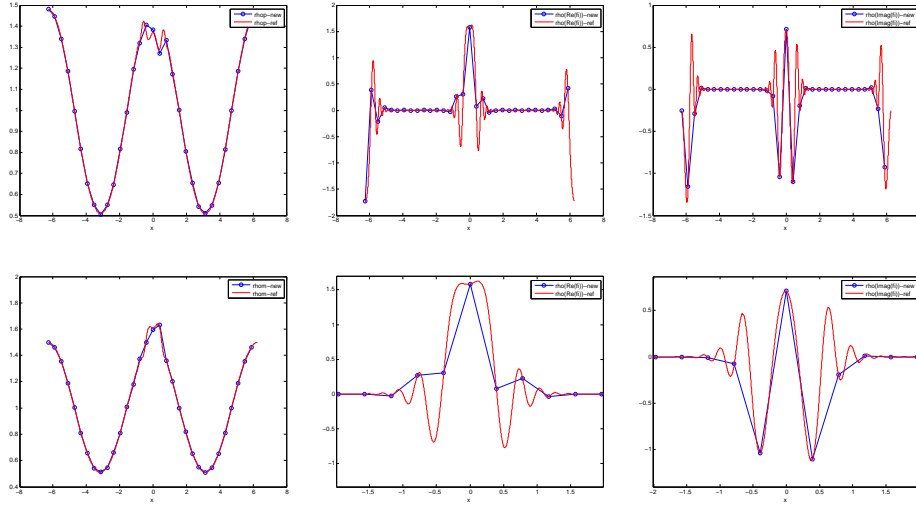

Figure 19: $\varepsilon = 1/256$. First line: space dependence of the densities ρ^+, $\mathrm{Re}(\rho^i)$ and $\mathrm{Im}(\rho^i)$. Second line: space dependence of ρ^-, $\mathrm{Re}(\rho^i)$ (zoom) and $\mathrm{Im}(\rho^i)$ (zoom).

[7] Philippe Chartier, Nicolas Crouseilles, Mohammed Lemou, and Florian Méhats, *Uniformly accurate numerical schemes for highly oscillatory Klein-Gordon and nonlinear Schrödinger equations*, Numer. Math. **129** (2015), no. 2, 211–250. MR 3300419

[8] Nicolas Crouseilles, Mohammed Lemou, and Florian Méhats, *Asymptotic preserving schemes for highly oscillatory Vlasov-Poisson equations*, J. Comput. Phys. **248** (2013), 287–308. MR 3066153

[9] Pierre Degond, *Asymptotic-preserving schemes for fluid models of plasmas*, Numerical models for fusion, Panor. Synthèses, vol. 39/40, Soc. Math. France, Paris, 2013, pp. 1–90. MR 3220424

[10] Ronald J. DiPerna and Andrew Majda, *The validity of nonlinear geometric optics for weak solutions of conservation laws*, Comm. Math. Phys. **98** (1985), no. 3, 313–347. MR 788777

[11] Weinan E and Bjorn Engquist, *The heterogeneous multiscale methods*, Commun. Math. Sci. **1** (2003), no. 1, 87–132. MR 1979846

[12] Björn Engquist and Olof Runborg, *Multi-phase computations in geometrical optics*, J. Comput. Appl. Math. **74** (1996), no. 1-2, 175–192, TICAM Symposium (Austin, TX, 1995). MR 1430373 (97k:78010)

[13] _____, *Computational high frequency wave propagation*, Acta Numer. **12** (2003), 181–266. MR 2249156 (2007f:65043)

[14] Erwan Faou, Vasile Gradinaru, and Christian Lubich, *Computing semiclassical quantum dynamics with Hagedorn wavepackets*, SIAM J. Sci. Comput. **31** (2009), no. 4, 3027–3041. MR 2520310

[15] E. Fatemi, B. Engquist, and S. Osher, *Numerical solution of the high frequency asymptotic expansion for the scalar wave equation*, J. Comput. Phys. **120** (1995), no. 1, 145–155. MR 1345031

[16] George A. Hagedorn, *Raising and lowering operators for semiclassical wave packets*, Ann. Physics **269** (1998), no. 1, 77–104. MR 1650826

[17] Eric J. Heller, *Frozen gaussians: a very simple semiclassical approximation*, Journal of Chemical Physics **75** (1981), 2923–2931.

[18] N. Ross Hill, *Gaussian beam migration*, Geophysics **55** (1990), no. 11, 1416–1428.

[19] Zhongyi Huang, Shi Jin, Peter A. Markowich, Christof Sparber, and Chunxiong Zheng, *A time-splitting spectral scheme for the Maxwell-Dirac system*, J. Comput. Phys. **208** (2005), no. 2, 761–789. MR 2144737

[20] Shi Jin, *Efficient asymptotic-preserving (AP) schemes for some multiscale kinetic equations*, SIAM J. Sci. Comput. **21** (1999), no. 2, 441–454 (electronic). MR 1718639

[21] _____, *Asymptotic preserving (AP) schemes for multiscale kinetic and hyperbolic equations: a review*, Riv. Math. Univ. Parma (N.S.) **3** (2012), no. 2, 177–216. MR 2964096

[22] Shi Jin and Xiantao Li, *Multi-phase computations of the semiclassical limit of the Schrödinger equation and related problems: Whitham vs. Wigner*, Phys. D **182** (2003), no. 1-2, 46–85. MR 2002860 (2004h:81136)

[23] Shi Jin, Peter Markowich, and Christof Sparber, *Mathematical and computational methods for semiclassical Schrödinger equations*, Acta Numer. **20** (2011), 121–209. MR 2805153

[24] Shi Jin and Stanley Osher, *A level set method for the computation of multivalued solutions to quasi-linear hyperbolic PDEs and Hamilton-Jacobi equations*, Commun. Math. Sci. **1** (2003), no. 3, 575–591. MR 2069944 (2005e:35152)

[25] Shi Jin and Peng Qi, *A hybrid Schrödinger/Gaussian beam solver for quantum barriers and surface hopping*, Kinet. Relat. Models **4** (2011), no. 4, 1097–1120. MR 2861588

[26] Shi Jin, Dongming Wei, and Dongsheng Yin, *Gaussian beam methods for the Schrödinger equation with discontinuous potentials*, J. Comput. Appl. Math. **265** (2014), 199–219. MR 3176269

[27] Shi Jin, Hao Wu, and Xu Yang, *Gaussian beam methods for the Schrödinger equation in the semi-classical regime: Lagrangian and Eulerian formulations*, Commun. Math. Sci. **6** (2008), no. 4, 995–1020. MR 2511703 (2010f:65217)

[28] Jean-Luc Joly, Guy Métivier, and Jeffrey Rauch, *Coherent and focusing multidimensional nonlinear geometric optics*, Ann. Sci. École Norm. Sup. (4) **28** (1995), no. 1, 51–113. MR 1305424

[29] Shingyu Leung, Jianliang Qian, and Robert Burridge, *Eulerian gaussian beams for high frequency wave propagation*, Geophysics **72** (2007), no. 2, 61–76.

[30] Jianfeng Lu and Xu Yang, *Frozen gaussian approximation for high frequency wave propagation*, Commun. Math. Sci. **9** (2011), 663–683.

[31] Andrew Majda, *Nonlinear geometric optics for hyperbolic systems of conservation laws*, Oscillation theory, computation, and methods of compensated compactness (Minneapolis, Minn., 1985), IMA Vol. Math. Appl., vol. 2, Springer, New York, 1986, pp. 115–165. MR 869824

[32] Victor P. Maslov and M. V. Fedoriuk, *Semiclassical approximation in quantum mechanics*, Mathematical Physics and Applied Mathematics, vol. 7, D. Reidel Publishing Co., Dordrecht-Boston, Mass., 1981, Translated from the Russian by J. Niederle and J. Tolar, Contemporary Mathematics, 5. MR 634377

[33] Omar Morandi, *Multiband wigner-function formalism applied to the zener band transition in a semiconductor*, Phys. Rev. B **80** (2009), no. 5-7, 024301. MR 2484386

[34] Omar Morandi and Ferdinand Schürrer, *Wigner model for quantum transport in graphene*, J. Phys. A **44** (2011), no. 5-7, 265–301. MR 2484386

[35] M. Popov, *A new method of computation of wave fields using Gaussian beams*, Wave Motion **4** (1982), no. 1, 85–97.

[36] James Ralston, *Gaussian beams and the propagation of singularities*, Studies in partial differential equations, MAA Stud. Math., vol. 23, Math. Assoc. America, Washington, DC, 1982, pp. 206–248. MR 716507 (85c:35052)

[37] Jeffrey Rauch and Markus Keel, *Lectures on geometric optics*, Hyperbolic equations and frequency interactions (Park City, UT, 1995), IAS/Park City Math. Ser., vol. 5, Amer. Math. Soc., Providence, RI, 1999, pp. 383–466. MR 1662833

[38] Christof Sparber, Peter A. Markowich, and Norbert Mauser, *Wigner functions versus WKB-methods in multivalued geometrical optics*, Asymptot. Anal. **33** (2003), no. 2, 153–187.

[39] Di Xiao, Ming-Che Chang, and Qian Niu, *Berry phase effects on electronic properties*, Reviews of Modern Physics **82** (2010), no. 3, 1959.